NASA TECHNICAL NOTE

NASA TN D-3604

NASA TN D-3604

SOME PRACTICAL ASPECTS OF SURFACE TEMPERATURE MEASUREMENT BY OPTICAL AND RATIO PYROMETERS

by J. Robert Branstetter

Lewis Research Center

Cleveland, Ohio

NATIONAL AERONAUTICS AND SPACE ADMINISTRATION • WASHINGTON, D. C. • SEPTEMBER 1966

NASA TN D-3604

SOME PRACTICAL ASPECTS OF SURFACE TEMPERATURE MEASUREMENT BY OPTICAL AND RATIO PYROMETERS

By J. Robert Branstetter

Lewis Research Center
Cleveland, Ohio

NATIONAL AERONAUTICS AND SPACE ADMINISTRATION

For sale by the Clearinghouse for Federal Scientific and Technical Information
Springfield, Virginia 22151 – Price $2.50

CONTENTS

SOME PRACTICAL ASPECTS OF SURFACE TEMPERATURE MEASUREMENT BY OPTICAL AND RATIO PYROMETERS

by J. Robert Branstetter

Lewis Research Center

SUMMARY

Techniques for obtaining the temperature of opaque materials by optical and ratio pyrometers are described. Fundamental equations of radiation are presented along with off-design corrections pertinent to pyrometer measurements. Characteristics of pyrometers both manual and automatic are discussed. Calibration apparatus and techniques are described. Techniques for minimizing temperature error resulting from small and/or awkardly located sources are analyzed. Also examined are the practical aspects of cavity-type sources. Precautions and procedures in the selection of emittance, reflectance, and transmittance data are included along with working curves helpful in deriving true temperatures from pyrometer-registered temperature readings.

INTRODUCTION

Many physical phenomena are extremely sensitive to temperature. An accurate experimental evaluation of such phenomena requires that the temperature be well defined. While the techniques available for measuring temperature are many, usually only one technique excels for any given set of circumstances. This report describes the apparatus and procedures for obtaining the surface temperatures of opaque objects by detectors that gather thermal radiant energy; this energy is presumed to be filtered by the sensing instrument so that only one or two relatively narrow bands of the energy spectrum are utilized.

In practice, the radiation characteristics of the object being measured significantly affect the accuracy of a radiation temperature measurement. The object is often small and subject both to spacial temperature gradients and to energy exchange with neighboring bodies. Techniques must be developed to cope with these problems.

Within the scope of this report, there exists a tremendous wealth of good literature.

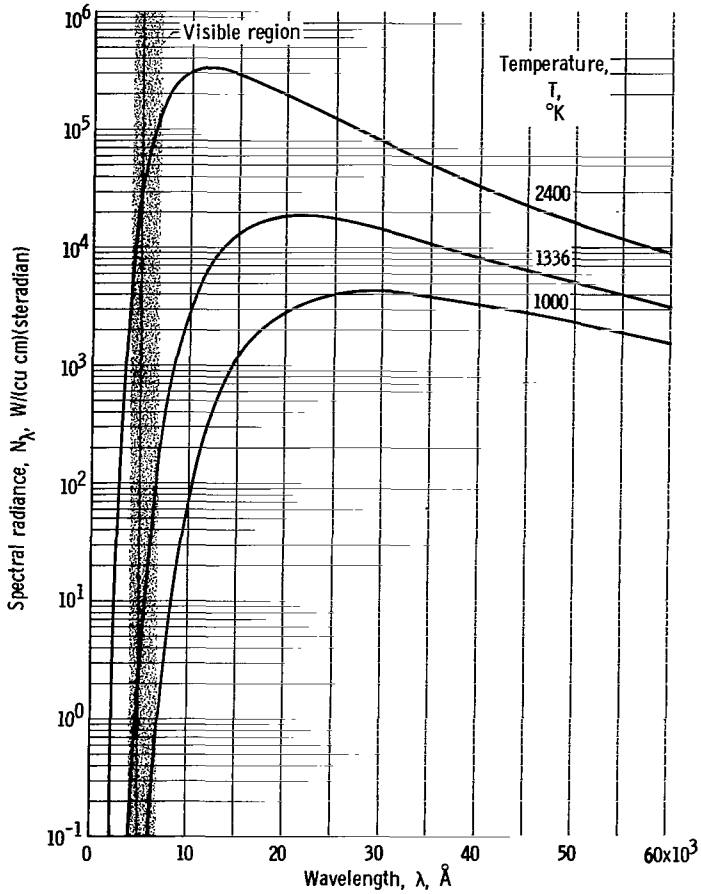

Figure 1. - Spectral radiance of blackbody.

Unfortunately, any one manuscript is devoted to only a portion of the whole task of making a temperature determination. Referenced material as well as results from experiments designed to fill some of the voids have been assembled herein to make available a collected body of applied technology and reference sources. Much of the material presented was obtained from references 1 and 2. The paper by Kostkowski and Lee (ref. 3, also included in ref. 1, p. 449) was also very valuable.

Because semantics in the realm of radiant energy leave much to be desired, many of the expressions used in this report are defined in appendix A. There are many types of emittances, reflectances, and transmittances, for example, total, spectral, normal, and hemispherical (ref. 4, p. 1164). Most attention herein is given to normal spectral emittance, and for this reason the descriptives "normal spectral" are usually omitted.

FUNDAMENTALS

Radiation Equations and Temperature Scale

The energy radiated by a blackbody is described by the Planck radiation equation

$$N_{\lambda,b} = \frac{C_1 \lambda^{-5}}{e^{C_2/\lambda T} - 1} \tag{1}$$

where $N_{\lambda,b}$ is spectral radiance (see glossary, appendix A, and symbols, appendix B). Radiance data for three temperatures are shown in figure 1.

The International Practical Temperature Scale (IPTS) of 1948 (ref. 5) defines the temperature T above the temperature of equilibrium between solid and liquid gold (gold point) T_G by the equation

$$\frac{N_{\lambda, b, T}}{N_{\lambda, b, T_G}} = \frac{e^{C_2/\lambda T_G} - 1}{e^{C_2/\lambda T} - 1} \tag{2}$$

where C_2 and T_G are defined as 1.438 centimeters-^{o}K and 1336.15^{o} K, respectively. Pyrometers calibrated at the National Bureau of Standards (NBS) are calibrated in terms of the IPTS (eq. (2)) for temperatures both higher and lower than the gold point (ref. 3).

The Wien approximation, because of its relative simplicity, is often used in place of the Planck equation. The Wien approximation,

$$N'_{\lambda, b} = \frac{C_1 \lambda^{-5}}{e^{C_2/\lambda T}} \tag{3}$$

closely matches $N_{\lambda, b}$ at short wavelengths and/or low values of T. Error incurred by use of the Wien equation at 6500 angstroms, as an approximation for the Planck equation in the IPTS, is shown in figure 2 (ref. 3). Also shown in the figure is the estimated difference between the Thermodynamic Temperature Scale (TTS, ref. 6) and the IPTS of 1948. This latter comparison is helpful when it is necessary to obtain a temperature on the TTS with an instrument calibrated on the IPTS.

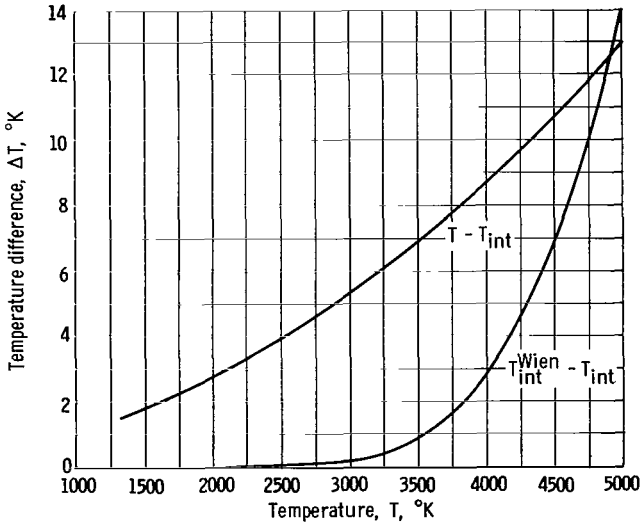

Figure 2. - Estimated difference between Thermodynamic Temperature Scale and International Practical Temperature Scale, and the error incurred when using the Wien equation (at 0.65 μ) as an approximation for the Planck equation in the International Practical Temperature Scale (ref. 3).

Temperature Corrections

The temperature of a source is obtained from the indicated temperature of a calibrated pyrometer in the following manner. An arbitrary source at temperature T and spectral emittance ϵ has a spectral radiance $N'_{\lambda, T}$ given by

Wien's equation as

$$N'_{\lambda, T} = \epsilon C_1 \lambda^{-5} e^{-C_2/\lambda T} \tag{4}$$

A blackbody at the same temperature T has a greater radiance, designated the blackbody radiance

$$N'_{\lambda, b, T} = C_1 \lambda^{-5} e^{-C_2/\lambda T} \tag{5}$$

and a blackbody having the same radiance $N'_{\lambda, T}$ has a lower temperature, designated the blackbody temperature T_b, where

$$N'_{\lambda, T} = C_1 \lambda^{-5} e^{-C_2/\lambda T_b} \tag{6}$$

Spectral emittance is defined as the ratio of spectral radiances of an arbitrary source to a blackbody source when both are at the same temperature; that is,

$$\epsilon = \frac{N'_{\lambda, T}}{N'_{\lambda, b, T}} \tag{7}$$

which is the ratio of equations (4) and (5).

The temperature correction for an optical pyrometer is given by equations (4) and (6) when the pyrometer has been calibrated by sighting on a blackbody source at temperature T_b so that the pyrometer indicated temperature is T_b. By equating (4) and (6) and taking the logarithm of the result, one obtains

$$\frac{1}{T} - \frac{1}{T_b} = \frac{\lambda}{C_2} \ln \epsilon \tag{8a}$$

The indicated temperature T_b hereinafter is called the "brightness temperature" S_B to avoid confusion in nomenclature between optical and ratio pyrometry (see appendix A). Hence,

$$\frac{1}{T} - \frac{1}{S_B} = \frac{\lambda}{C_2} \ln \epsilon \tag{8b}$$

Since equations (8) contain the reciprocal of the temperature, it is convenient to discuss first the correction in $1/S_B$ that can be subsequently converted to a correction in S_B. By writing $\frac{1}{T} - \frac{1}{S_B}$ as E_B (the correction in $1/S_B$), one obtains

$$E_B = \frac{\lambda}{C_2} \ln \epsilon \tag{9}$$

This is the correction equation for the optical pyrometer, where $C_2 = 1.438$ centimeters-^{o}K, and λ is the wavelength in angstroms $\times 10^{-8}$. Note that E_B varies with both λ and ϵ. For example, if the wavelength λ is 6500 angstroms, the emittance ϵ is 0.418 (at wavelength λ and temperature T), and the brightness temperature S_B is 2681^{o} K, the correction factor is

$$E_B = \frac{6500 \times 10^{-8}}{1.438} \ln 0.418 = -3.94 \times 10^{-5}$$

Hence,

$$\frac{1}{T} = \frac{1}{2681} - 3.94 \times 10^{-5}$$

or

$$T = 3000^{o} \text{ K}$$

Corrections for other combinations of temperature, emittance, and wavelength may be computed in the same manner.

Temperature correction for a two-color pyrometer is given by equations (4) and (6) written for two wavelengths when the pyrometer has been calibrated in terms of a blackbody source at temperature T_b so that the pyrometer indicated temperature is T_b. The ratio of equations (4) and (6) is

$$\frac{N'_{\lambda_1, T}}{N'_{\lambda_2, T}} = \frac{\epsilon_1 C_1 \lambda_1^{-5} e^{-C_2/\lambda_1 T}}{\epsilon_2 C_1 \lambda_2^{-5} e^{-C_2/\lambda_2 T}} = \frac{C_1 \lambda_1^{-5} e^{-C_2/\lambda_1 T_b}}{C_1 \lambda_2^{-5} e^{-C_2/\lambda_2 T_b}} \tag{10}$$

The equality on the right can be reduced to

$$\frac{\epsilon_1 e^{-C_2/\lambda_1 T}}{\epsilon_2 e^{-C_2/\lambda_2 T}} = \frac{e^{-C_2/\lambda_1 T_b}}{e^{-C_2/\lambda_2 T_b}} \tag{11}$$

By taking the logarithm of the equation and rearranging terms, one obtains

$$\ln \frac{\epsilon_1}{\epsilon_2} = -C_2\left(\frac{1}{\lambda_2} - \frac{1}{\lambda_1}\right)\left(\frac{1}{T} - \frac{1}{T_b}\right) \tag{12a}$$

For this pyrometer, T_b hereinafter is called the "color" temperature S_C (see appendix A). Then

$$\ln \frac{\epsilon_1}{\epsilon_2} = -C_2\left(\frac{1}{\lambda_2} - \frac{1}{\lambda_1}\right)\left(\frac{1}{T} - \frac{1}{S_C}\right) \tag{12b}$$

The correction in $1/S_C$ for color temperature can be written as

$$\frac{1}{T} - \frac{1}{S_C} \equiv E_C = -\frac{\lambda_1 \lambda_2}{C_2(\lambda_1 - \lambda_2)} \ln \frac{\epsilon_1}{\epsilon_2} \tag{13}$$

This is the correction equation for the ratio pyrometer. Please observe that the sign of E_C is determined by the relative magnitudes of ϵ_1 and ϵ_2. For many refractory materials, the emittance at the longer wavelength has the smaller value, which in turn makes E_C a positive number and results in S_C values that are larger than T values. In contrast, values of S_B are always smaller than values of T.

Alternate Method of Making Temperature Corrections

The Wien approximation usually yields a trivial error (see fig. 2); however, exact solutions for E_C and E_B require that the more cumbersome Planck equation be used. Tables of reference 7 based on the IPTS of 1948 are well suited for exact solutions.

Appendix C describes and presents charts for obtaining T from S_B and S_C for several selected values of wavelength. Values of effective emittance ϵ' are used as the parameter on these charts. For the purpose of discussing the material presented thus far, ϵ' can be interpreted as ϵ. The charts are otherwise self-explanatory.

Influence of Uncertainty in Value of Emittance on Temperature Corrections

The influence of an inaccuracy in emittance values on the inaccuracy of the temperature values is now examined (ref. 8). In the case of the optical pyrometer, a differentiation of equation (8) and elimination of the second-order term yield

$$\beta_B = \frac{T\lambda\gamma_B}{C_2} \tag{14}$$

where β_B is the percent uncertainty in the value T, and γ_B is the percent uncertainty in the value ϵ. As an example, at a wavelength of 6500 angstroms, a 2-percent error in the value of emittance yields a 4° error in the value of T if T is near 2000° K.

In the case of the ratio pyrometer, a differentiation of equation (12) and elimination of the second-order term yield

$$\beta_C = \frac{\pm 2T\lambda_1\lambda_2\gamma_C}{(\lambda_1 - \lambda_2)C_2} \tag{15}$$

where β_C is the percentage uncertainty in the value of T, and γ_C is the percentage uncertainty in each of the emittances ϵ_1 and ϵ_2. The uncertainty in ϵ_1 is assumed to be equal in magnitude and opposite in sign to that of ϵ_2; hence, β_C is a maximum uncertainty.

A comparison of equations (14) and (15) for typical wavelengths shows that the maximum uncertainty of β_C is approximately sixfold greater than that of β_B. Hasty interpretation of these results can be misleading. For example, if the percentage uncertainties in values of ϵ_1 and of ϵ_2 happen to be equal both in magnitude and sign, the uncertainty in temperature β_C would be zero. Also, if ϵ_1 happens to equal ϵ_2, T would equal S_C. These results are also obvious from equation (13).

The uncertainty in the value of source emittance is not the only factor that an experimenter should take into account when he compares the relative error of optical and ratio pyrometers. Stray radiant energy from other than target sources that reflects from the

target and into the pyrometer is equivalent to a perturbation of target emittance. Furthermore, if the absorption of the intervening media is not the same for the two wavelength intervals of a ratio pyrometer, the indicated temperature may be far removed from the target temperature. Hill (ref. 2, p. 419) states that no ratio pyrometer can be regarded as universally applicable for all temperature measurement problems. Each application must be considered for characteristic pitfalls that can make a ratio pyrometer virtually useless. He notes that it is most desirable that a ratio pyrometer possess sufficient flexibility to permit selecting valid wavelength intervals for specific applications.

Influence of Deviation from Constant or Discrete Wavelength on Temperature Corrections

The ideal pyrometer (which has been the subject of discussion so far) senses radiation only at the prescribed wavelength. However, to be detectable, a nonzero bandwidth of radiation is needed. Visual optical pyrometers, in particular, require a rather large spectral bandwidth in order to have sufficient energy for effective detection. Reference 3 details the technique by which the effective wavelength (the value of λ in eq. (9)) of a visual optical pyrometer can be determined.

Both optical and ratio pyrometers that employ physical detectors usually have smaller spectral bandwidths than visual pyrometers; however, some instruments, in an endeavor to register signals from low-temperature sources, have bandwidths sufficiently wide to cause concern. On request, instrument manufacturers will provide effective wavelength data.

Since the effective wavelength of pyrometers varies with temperature and with the manufacturer, it is good practice to determine if temperature conversion charts prepared for a particular wavelength are sufficiently accurate for the intended use of a particular pyrometer. While the charts presented in appendix C are correct only for the wavelengths designated therein, a simple approximation can permit the use of these charts at other values of wavelength. A method of determining the temperature T from a value of S obtained at an off-design value of λ is as follows: The previously used expression

$$\frac{1}{T} - \frac{1}{S} = E \tag{16}$$

by rearrangement becomes

$$T - S = -\frac{ES^2}{ES + 1} \tag{17}$$

Only a small error is incurred by letting

$$T - S = -ES^2 \tag{18}$$

Now for a given pyrometer reading S, the ratio of the correction at wavelength λ_p to the correction at wavelength λ_q, can be written as

$$\frac{(T - S)_p}{(T - S)_q} = \frac{E_p S^2}{E_q S^2} = \frac{E_p}{E_q} \tag{19}$$

(This equation is applicable for both optical and two-color pyrometers.)

For example, a brightness temperature reading of 2050° K exists at an effective wavelength of 6000 angstroms. Also, at this wavelength, the emittance of the source is 0.55. The true temperature is desired.

For a constant value of ϵ, equation (9) shows E_B to be directly proportional to λ. Therefore,

$$\frac{E_{B,\,6000}}{E_{B,\,6530}} = \frac{6000}{6530} = 0.92$$

where 6530 is a reference wavelength used in figure 30(a). Therein, at 6530 angstroms and at an emittance of 0.55, the value of T - S is 120° K. Thus, from equation (19), one obtains

$$(T - S)_{6000} = 120 \times 0.92 = 110^{\circ} \text{ C}$$

Hence, the true temperature is 2160° K.

In a similar manner, an adjustment to color temperature for nonstandard wavelength can be obtained by using the color temperature charts and equations (13) and (19).

GENERAL DESCRIPTION OF PYROMETERS

In the material presented thus far, it has been tacitly assumed that data in the form of S_B or S_C had already been gathered, that emittance and wavelength values were known, and that the only task at hand was to evaluate T.

To obtain accurate values of indicated temperature S, the experimenter must be

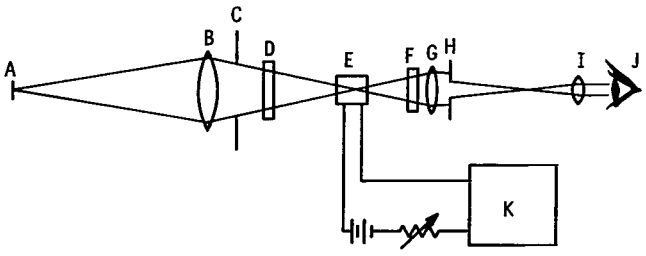

A, Source
B, Objective lens
C, Objective aperture
D, Absorption filter (used for temperature above 1300° C)
E, Pyrometer lamp
F, Red filter
G, Microscope objective lens
H, Microscope aperture stop
I, Microscope ocular
J, Eye
K, Current measuring instrument

Figure 3. - Schematic diagram of optical pyrometer (ref. 3).

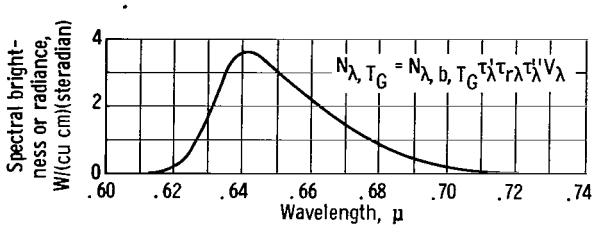

Figure 4. - Spectral brightness of gold-point blackbody N_{λ, T_G} as seen by observer with relative luminosity function V_λ through an optical pyrometer. Spectral transmittances: $\tau_{r\lambda}$ for red glass; $\tau_\lambda' = 0.8$ and $\tau_\lambda'' = 0.7$ for all optical elements preceding and following pyrometer lamp filament, respectively, excluding red glass (ref. 3).

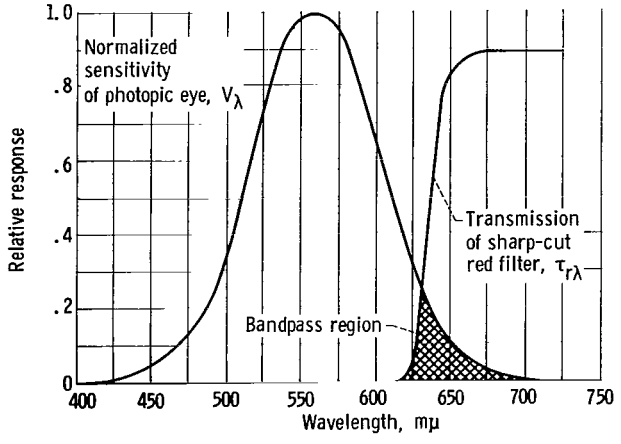

Figure 5. - Narrow pass filter of conventional brightness pyrometer (ref. 2, p. 866).

thoroughly acquainted with his pyrometer. A general description of several classes of pyrometers is presented in the following sections.

Visual Optical Pyrometers

A typical disappearing-filament pyrometer is shown in the schematic diagram in figure 3, which was obtained from reference 3. The instrument is operated by imaging the source (target), whose temperature is to be determined, onto the filament of the small pyrometer lamp and varying the current in this lamp until its filament disappears into the background of the source. At this time the photometric brightness of the body and the pyrometer lamp filament, as seen through the optical pyrometer, are the same. The spectral photometric brightness of a blackbody at the gold point as seen by an observer is shown in figure 4 (ref. 3). The spectral photometric brightness expressed in units of spectral radiance is

$$N_\lambda = N_{\lambda, b} \epsilon \tau V_\lambda$$

where τ is the spectral transmission of all optical elements of the pyrometer, and V_λ is the relative luminosity function of the eye. The red filter of the instrument serves to cut off the energy at short wavelengths, and the eye cuts off the

long-wavelength energy (see fig. 5). This is the type of pyrometer the NBS uses to realize and distribute the IPTS. The effective wavelength of the NBS optical pyrometer ranges in abrupt changes from 6530 to 6570 angstroms over a temperature range of 800° to 2300° C. The NBS reports (ref. 3) "Most of the visual optical pyrometers received for calibration that have been manufactured since about 1959 appear to have mean effective wavelengths negligibly different from those of the NBS instrument. However, this is not the case for the older instruments. Some of these had differences as large as 0.01μ, corresponding to about a 5° C correction at a tungsten brightness temperature of 2400° C and to about a 1° C correction at 1063° C."

Status of visual optical pyrometry is reviewed by Lovejoy (ref. 1, p. 487) and by Kostkowski and Lee (ref. 3). The referenced authors generally agree that the fundamental limitation in these instruments is the sensitivity of the human eye; however, optical contrast techniques are available (refs. 3 and 9) that may possibly provide greater precision and accuracy than are now reported for visual optical pyrometers.

Photoelectric Optical Pyrometers

In principle, the photoelectric optical pyrometer has considerably greater sensitivity and precision than visual instruments and can use a much smaller spectral bandwidth. A number of different types of photoelectric optical pyrometers are described in reference 1 (pp. 507, 517, and 523) and reference 2 (pp. 865 and 873). A schematic diagram of one such instrument is shown in figure 6 (ref. 2, p. 865). A revolving mirror alternately scans the target and the reference source at high speed. The optical system thus projects alternately an image of the target and of the reference source onto the photomultiplier. One technique for determining temperature is to adjust the reference lamp current manually or automatically until a null intensity is sensed in the photomultiplier output current. Such an instrument is slower than one in which the lamp current is maintained constant and the temperature is sensed by an off-balance meter reading. One of these latter type pyrometers is described in reference 2 (p. 867). When either type of instrument is self-stabilizing and provides

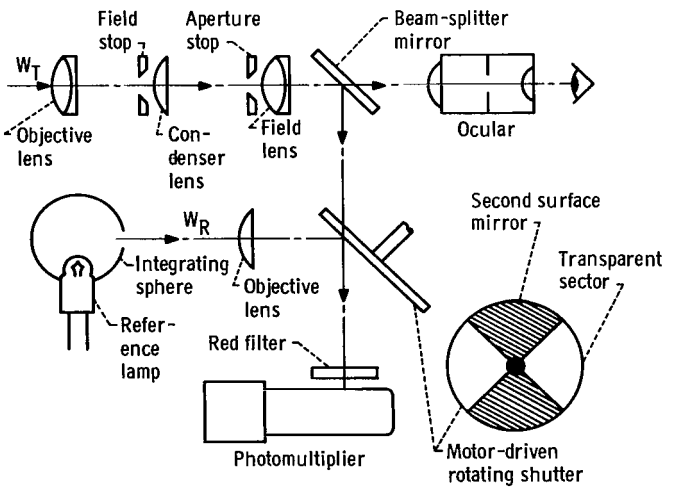

Figure 6. - Optical diagram of typical automatic brightness pyrometer (ref. 2, p. 865).

direct readout of temperature, it is commonly referred to as being automatic. Automatic pyrometers can be readily adapted to recorder and controller facilities.

At low temperatures, the radiance of a source (fig. 1, p. 2) is relatively small in the visible wavelength region. Reference 1 (p. 501) notes that "In the past, optical pyrometry has come to be based on a standard wavelength of 0.65μ. However, many of the newer photodetectors have their sensitivity peaks at longer wavelengths, for example, at 1.0 micron for S1 photoemissive detectors, 1.6 micron for germanium phototransistors, 2.5 micron for lead sulfide photoconductive cells and 4.0 micron for cooled lead telluride photoconductive cells." Modern detectors permit the measurement of very low temperatures. By removing the filters and sensing heat rather than spectral radiance (this would be a total radiation pyrometer) source temperature as low as 100^{o} C can be measured.

It is expected that photoelectric pyrometry will make possible at least an order of magnitude greater accuracy in optical pyrometry (ref. 3). Toward this end the NBS is developing a high-accuracy photoelectric instrument (ref. 1, p. 507).

Ratio Pyrometers

Several ratio pyrometers, operated automatically or otherwise, are described in reference 2; however, the scope of the present report is limited to automatically oper-

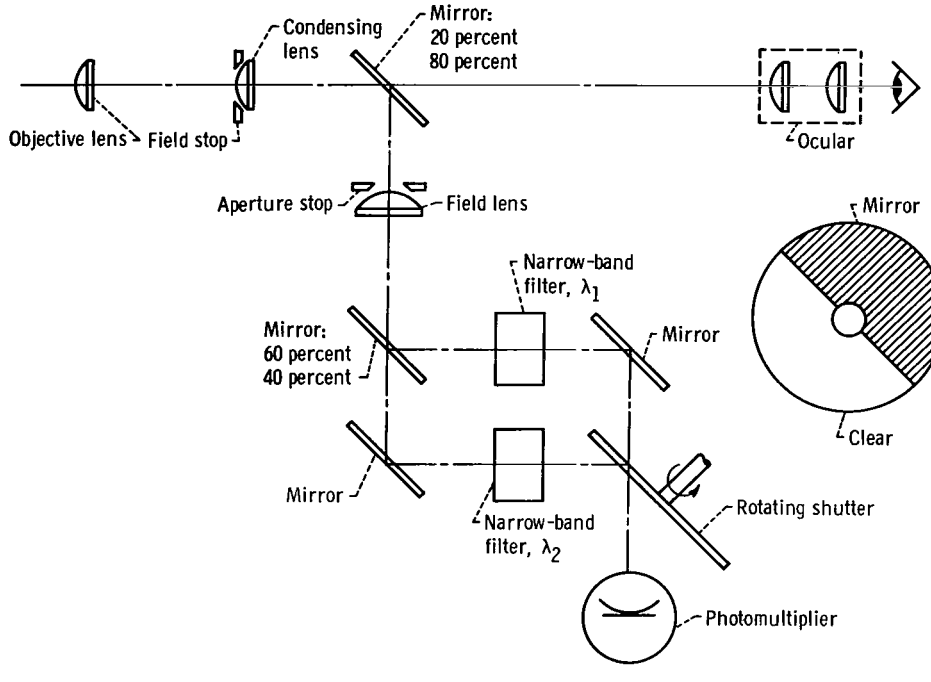

Figure 7. - Optical diagram of two-color pyrometer (ref. 2, p. 850).

ated two-color pyrometers. The optical diagram of one such instrument is shown in figure 7 (ref. 2, p. 849). In principle, it operates in the following manner: An ideal photomultiplier viewing a source unrestricted by the optical system except for ideal narrow-band filters at wavelengths λ_1 and λ_2 would alternately sense the numerator and denominator of equation (10), namely

$$N'_{\lambda_1, T} = \frac{\epsilon_1 C_1 \lambda_1^{-5}}{e^{C_2/\lambda_1 T}} \tag{20a}$$

and

$$N'_{\lambda_2, T} = \frac{\epsilon_2 C_1 \lambda_2^{-5}}{e^{C_2/\lambda_2 T}} \tag{20b}$$

It is well to emphasize that, in this idealized case, the product of the detector response and the transmittance of optical glass within each band has a value of 1. Dividing equation 20(a) by equation 20(b) and simplifying the result in a manner similar to the derivation of equation 12(b) give

$$\frac{N'_{\lambda_1, T}}{N'_{\lambda_2, T}} \equiv R_o = \left(\frac{\lambda_2}{\lambda_1}\right)^5 \exp\left[\frac{C_2}{S_C}\left(\frac{1}{\lambda_2} - \frac{1}{\lambda_1}\right)\right] \tag{21}$$

where R_o is the ratio of the two signals incident upon the photodetector and is shown to be dependent on S_C.

Equations based on real optics and electronic devices are described in reference 2 (p. 849) along with design and performance characteristics. Even more so than in the case of optical pyrometers, filters possessing narrow transmission bands are necessary to ensure good accuracy. Well-defined values of wavelength are required in equation (13) for precise conversion of S_C values to T values. Also, reference 2 (p. 853) reports that it is possible to design, adjust, and apply discrete filter instruments with a higher degree of predictability and with a minimum complexity of computation. The principal disadvantage of discrete filters is that they transmit a very small quantity of energy at temperatures below about 850° C.

The signal to noise ratio of a ratio pyrometer is improved by making the quantity

$\left|\frac{1}{\lambda_2} - \frac{1}{\lambda_1}\right|$ of equation (21) as large as possible (ref. 2, p. 853); however, spectral radiance at short optical wavelengths is very small.

High-Speed Pyrometers

The speed at which temperature can be measured with a photoelectric pyrometer is governed by several factors. As mentioned earlier, pyrometers employing lamps, in which current is varied to obtain a brightness match, are basically low-speed devices. This problem occurs neither with optical pyrometers utilizing constant current lamps nor with ratio pyrometers. For these latter two instruments, the basic limit on response time is the noise level of the detector and the maximum output noise level that can be tolerated. "Clean" electronics are most desirable at low signal strength, that is, low temperature and/or small field of view. Direct coupling of the photodetector to an oscilloscope or magnetic tape permits millisecond data gathering; however, this technique requires extensive data-reduction efforts. Pyrometers whose circuitry provides direct readout of temperature are considerably slower. The response time of several ammeter-type temperature-display pyrometers currently being offered on the market is about 1 second. Incidentally, these pyrometers usually employ several partially overlapping temperature scales in order to expand the meter scale. Scale switching is done manually.

PYROMETER CALIBRATION

The calibration of a pyrometer can be done in any of several ways. A primary calibration facility can be set up to realize the IPTS (eq. (2)) directly. If a person performs a primary calibration with a carefully designed and constructed pyrometer and with all the precautions taken at a national standards laboratory, it is possible to approach the accuracy listed in table I obtained from Kostkowski and Burns (ref. 10, p. 13). Secondly, the NBS provides calibration services. Fees and instructions are listed in the Federal Register. Lastly, there are a variety of methods for calibrating one's own instruments by means of NBS standards, which are available in the form of tungsten strip lamps, visual optical pyrometers, and arc lamps. These secondary standards will be discussed along with procedures and apparatus pertinent to pyrometer calibration.

Certified Tungsten Strip Lamps

Vacuum strip lamps are generally more stable than gas-filled lamps below temper-

TABLE I. - ESTIMATED ACCURACY[a] AND PRECISION[b] IN ^{o}C OF TEMPERATURE SCALES AS OF 1962 (REF. 10)

Temperature (Int. 1948), ^{o}C	Estimated accuracy of realizing International Practical Temperature Scale of 1948	Estimated precision of thermometers used to realize International Practical Temperature Scale of 1948
630.5	[c]0.02	[c]0.002
	.2	.1
960.8 (silver point)	.2	.1
1063 (gold point)	[d].2	[d].1
	.4	.3
2000	2	1
4000	10	3

[a]Accuracy here means estimated standard deviation of the mean of determinations from each laboratory in which attempts have been made to realize either the international or the thermodynamic temperature scales about the mean of all laboratories.

[b]Precision of a thermometer means the estimated standard deviation of the determinations of any laboratory (using one thermometer) about the mean of the determinations in the same laboratory.

[c]The first of the two entries (0.02) refers to a standard platinum resistance thermometer and the second (0.002) to a standard thermocouple.

[d]The two entries are standard thermocouple and visual optical pyrometer, respectively.

atures of about 1400^{o} C and should be used in preference to gas-filled lamps whenever possible (ref. 3).

The lamps used at Lewis are type 30A/6V/T24 manufactured by the General Electric Company. They are nominally rated at 6 volts and 30 amperes, are gas-filled, and have a 3-inch-diameter tubular glass envelope with a clear selected window. The ribbon filament is 3 millimeters wide, 50 millimeters long, mounted laterally off the axis, and notched at the point of sighting. The maximum operating temperature recommended by NBS is 2300^{o} C brightness temperature.

A strip lamp that is especially useful when a higher brightness temperature is required is the General Electric 75A/T24 (ref. 3). The filament and filament supports of this lamp are designed for use up to a brightness temperature of about 2800^{o} K. In addition, the lamp may be obtained with a plain quartz window so that it can be used in the ultraviolet spectral region. However, these lamps require about twice the current of the 30A/6V/T24 lamp and have no notch. Reference 3 also describes other tungsten strip lamps.

The calibration procedure used by NBS for strip lamps is well documented in

Form NBS-495
(Rev. 9-1-60)

UNITED STATES DEPARTMENT OF COMMERCE
WASHINGTON 25, D.C.

National Bureau of Standards Certificate

Ribbon Filament Lamp

Submitted by

National Aeronautics and Space Administration
21000 Brookpark Road
Cleveland, Ohio

Brightness Temperature (at 0.653 micron) versus Lamp Current

Degrees C (Int. 1948)	Amperes (abs.)	Degrees C (Int. 1948)	Amperes (abs.)
800	11.26	1600	23.53
900	12.12	1700	25.78
1000	13.17	1800	28.13
1100	14.44	1900	30.58
1200	15.92	2000	33.12
1300	17.59	2100	35.75
1400	19.43	2200	38.48
1500	21.41	2300	41.30

The maximum uncertainties of the values at 1000 °C and at 1100 °C correspond to about ± 3 degrees. At higher and lower temperatures the maximum uncertainties are larger, increasing to about ± 5 degrees at 800 °C and to about ± 7 degrees at 2300 °C.

These values apply when the lamp is operated base down and the portion of the filament at the notch made vertical. The center contact should be at a positive potential and the room temperature at 25 °C. The sighting should be made on the center of the filament across from the notch, with the arrow, etched on the back of the envelope, appearing at the notch. The magnitude of the effect when altering these conditions can be obtained from the paper, "Factors Affecting the Reproducibility of Brightness of Tungsten Strip Lamps for Pyrometer Standardization," by C. R. Barber, J. Sci. Inst. **23**, 238 (1946).

Sightings were made such that the angle subtended at the lamp filament by the entrance pupil of the pyrometer was 0.02 radian in the range 1100 °C to 2300 °C, 0.03 radian at 1000 °C, 0.04 radian at 900 °C, and 0.05 radian at 800 °C.

For the Director

Henry J. Kostkowski

Henry J. Kostkowski
High Temperature Measurements Laboratory
Heat Division

P.O. No. C-91187
Test No. G32198A
Date: Feb. 15, 1963
EL/mr

U.S. GOVERNMENT PRINTING OFFICE 666916

Figure 8. - Typical certificate for type 30A/6V/T24 tungsten strip lamp.

reference 3. A typical certificate (fig. 8) shows accuracy estimates and pertinent operating instructions. While the brightness temperatures are reported (fig. 8) to correspond to a wavelength of 6530 angstroms, the actual wavelength for the observations between 800° and 2300° C varied from 6570 to 6530 angstroms with abrupt changes in wavelength whenever the range of the NBS pyrometer was changed. However, the greatest difference in the actual wavelength and that reported only amounts to an error in brightness temperature of about one-seventh the uncertainty stated. The NBS first orients the lamp, etches the arrow, and anneals the filament. The first temperature calibrated is at the highest point requested. In the usual case of calibrating at intervals of 100° C, the observers wait 10 minutes between points to allow the lamp to reach equilibrium after each temperature change. However, at 1000° and 900° C, a 15-minute wait is employed; at 800° C, 20 minutes. For temperature changes greater than 100° C, even longer waiting periods are used.

The electrical system used by the NBS to calibrate a lamp employs storage batteries, a specially constructed air-ventilated resistor, and a control and measuring system that provides amperage accuracy of 1 part in 10 000 (ref. 3). A strip-lamp installation used by Lewis is shown in figures 9 and 10. It operates on a 60-cycle single-phase 115-volt supply. The single-rack system is portable and requires no maintenance due to long periods of downtime. A direct-current voltage rectifier (mounted out of view in fig. 10) provides a regulated output over a manually selected range of 9 to 18 volts. Line regu-

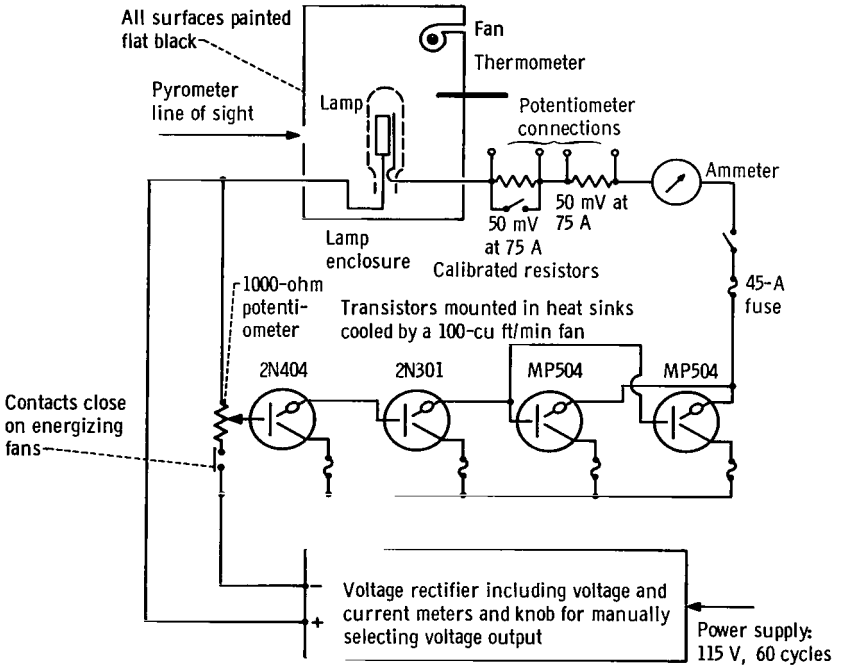

Figure 9. - Schematic diagram of electrical system for strip lamp. Nominal rating, 30 amperes at 6 volts.

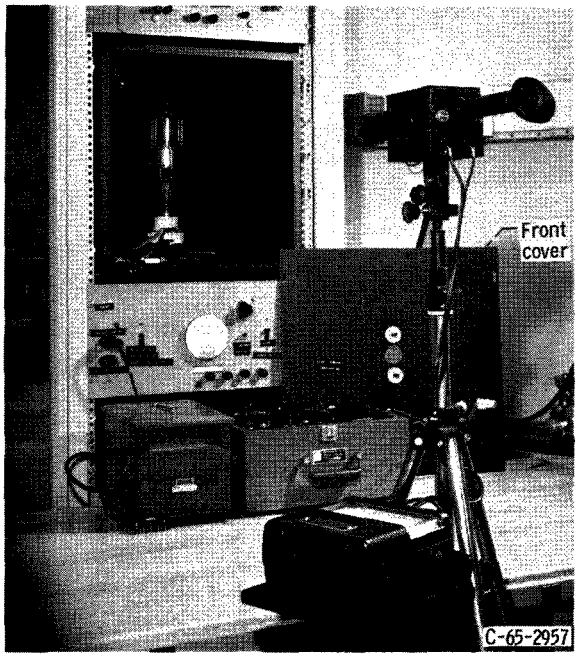

Figure 10. - Pyrometer sighted on strip lamp. Front cover has been removed so that lamp assembly can be seen.

lation is ±0.1 percent, load regulation is ±0.2 percent, ripple is approximately 1.0 percent, and response is 0.15 second. The rated output current is 60 amperes (at 14 V). A manually operated, 10-turn, 1000-ohm pot, used as a bias in conjunction with a bank of transistors, provides (1) fine-voltage adjustment and (2) a means of obtaining lamp voltages smaller than the minimum voltage provided by the rectifier. For 30A/6V/T24 lamps, a voltage-rectifier output of about 14 volts is required to obtain a brightness temperature of 2300° C; however, at currents below 30 amperes, the output potential of the voltage rectifier itself is kept below 10 volts to prevent the transistors from overheating. Otherwise, fixed-current settings are obtained by adjusting the transistor bias. Unattended, the system will hold the brightness temperature constant to within 1° K of the set value for hours. It proved convenient to mount the lamp on a rack and pinion base so that the distance between the lamp and the pyrometer could be varied without shifting and hence misalining the tripod-mounted pyrometer.

Pyrometric Arc Lamps

A graphite arc of the prescribed type when operated at specified conditions provides a fairly stable temperature source approaching that of a blackbody (see ref. 1, p. 551). One such commercially available arc lamp is described in reference 11. The brightness temperature (6500 Å) of this lamp, when 1/4-inch-diameter positive electrodes are used, is stated to be 3803° K. The lamp is easy to operate especially when the 1/4-inch-diameter rod is used. NBS certified filter glasses may be obtained from the lamp manufacturer for set values of brightness temperatures as low as 1300° K. Long-term variation of the lamp without filters is 12° C. With filters, the brightness temperature has a maximum uncertainty of the order of 1 percent. (An alternate method of reducing brightness of the source is to use a sectored disk.)

Certified Pyrometers

Several disappearing-filament optical instruments on the market today are well suited as reference pyrometers. Good quality visual pyrometers are stable in operation and can be used for precise measurements. The focus is crisp. The optics are designed for distance compensation, hence, calibration does not change appreciably as the distance between the instrument and the source is varied. The time to reach equilibrium ranges from seconds to 1 minute. Since the temperature equilibration time of a source increases with the size of the radiation source, pyrometers that require large targets to establish accurate readings are to be avoided. As emphasized in earlier sections of this report, the effective wavelength of the instrument should be reasonably constant with temperature and should be near 6530 angstroms.

The NBS provides pyrometer calibration services for temperatures ranging from 800° to above 4000° C. Reference 10 (p. 25) states "For optimum precision and accuracy in the use of optical pyrometers, laboratories should request NBS to calibrate their pyrometers as a function of pyrometer filament current. The laboratory should use a standard resistor and a sufficiently accurate potentiometer to determine this current. A multi-turn smooth-turning rheostat is highly desirable for varying the filament current while making brightness matches."

As of 1961, certified pyrometers of good quality had calibration accuracies about the same as those of strip lamps (fig. 8, p. 16).

Comparison Radiation Sources

When a reference pyrometer is used to calibrate a second pyrometer, the source on which they are sighted must be chosen with considerable care. A tungsten strip lamp provides an inexpensive and relatively fast responding comparison source; however, strip lamps have several limitations. The emittance of an annealed tungsten surface varies appreciably both with temperature and wavelength. The emittance is well defined only for specially prepared surface finishes. Radiance with direction of view varies because of multiple reflections between the filament and the glass envelope. Hence, the true temperature T of the filament cannot be determined to a high degree of accuracy. As a result, a strip lamp is a reliable comparison source only for calibration of a brightness pyrometer that possesses an effective wavelength nearly equal to that of the reference pyrometer. When a strip lamp is used, the filament should be notched and the lamp oriented and alined with care similar to that for certified-lamp procedure.

If a blackbody is the comparison source, the brightness temperature is independent of wavelength (eq. (9)), and in fact S_B, S_C, and T are equal to each other. A number

of furnaces possessing near-blackbody emittance are described in the literature (refs. 3, 10, p. 408; ref. 12, p. 233; and ref. 13). Also, several furnace manufacturers produce small open-ended furnaces that are advertised as being nearly black.

Procedures

Both tungsten strip lamps and small lamps in optical pyrometers change with use. Therefore, in order to obtain high accuracy, a laboratory should use a certified strip lamp or a certified optical pyrometer infrequently and compare it with the strip lamps or pyrometers used regularly. For best accuracy, certified reference pyrometers should be recalibrated (as a function of pyrometer current) after about 200 hours of use. Calibration of gas-filled reference strip lamps should be checked more frequently. Close adherence to the instructions contained in the NBS certification is most desirable. The magnitude of likely errors incurred by off-design use is described in references 3 and 14.

Several items regarding the use of optical pyrometers are worthy of emphasis. Precision of matches can often be improved greatly by having the pyrometer mounted rigidly in a comfortable position for a sitting observer. A black cloth thrown over the observer's head and part of the pyrometer to shield the observer from any distracting or annoying light is helpful. Observations should always be made from both a dark and a bright filament to a match (or disappearance) and the two results averaged. Also, the luminosity factor V_λ varies from one person to the next. Usually this difference is small; however, it is good practice for an observer who is using nonblackbody sources to determine if he does have an unusual relative luminosity curve. This can be done by comparing the results of five or six observers. When lamps are being sighted on, it is a common failing for the operator to attempt readings before the lamp temperature has stabilized.

A laboratory that desires to maintain a secondary standard of the IPTS for the purpose of calibrating pyrometers can select, from the apparatus described previously, the equipment that most nearly matches its particular need. Experiences at Lewis can be cited. Calibration facilities were required for both ratio and optical pyrometers. Also one of the optical pyrometers had an effective wavelength of 5330 angstroms; however, most of the pyrometers were of the disappearing-filament type with effective wavelengths near 6530 angstroms. These latter instruments were calibrated by direct-sighting on a certified lamp (fig. 10). Periodically, a check of this frequently used certified lamp was obtained as follows: A particularly careful calibration was conducted on a good quality visual pyrometer. Then the strip lamp was replaced by an infrequently used certified lamp, which was then examined to determine if the aged lamp had changed calibration.

The particular pyrometer employed to check the strip lamp was used to calibrate all pyrometers not of the 6530-angstrom optical type. The check was accomplished by

mounting the two pyrometers side by side and sighting them on the inductively heated graphite furnace shown in figure 11 and described in reference 13. The cavity had a diameter of 0.9 centimeter and a temperature limit of 3000° K. The cavity emittance was taken to be 1, and there was no absorbing media such as glassware between the furnace and the pyrometers. Hence, the tasks of obtaining the effective wavelength and the correction E were eliminated. It should be noted that the target areas of the furnace and the strip lamp described herein are too small for some pyrometers currently on the market.

ACCURACY, PRECISION, AND STABILITY OF PYROMETERS

The accuracy of a pyrometer is subject to many factors, a number of which have been developed in the preceding sections. It was shown that pyrometers when sighted on blackbody sources exhibit their greatest accuracy. In this section, accuracy, precision, and stability (long-term drift) will be discussed by assuming the following idealized conditions: (1) blackbody source, (2) free, unhindered view of the source, and (3) source of ample size and uniform temperature.

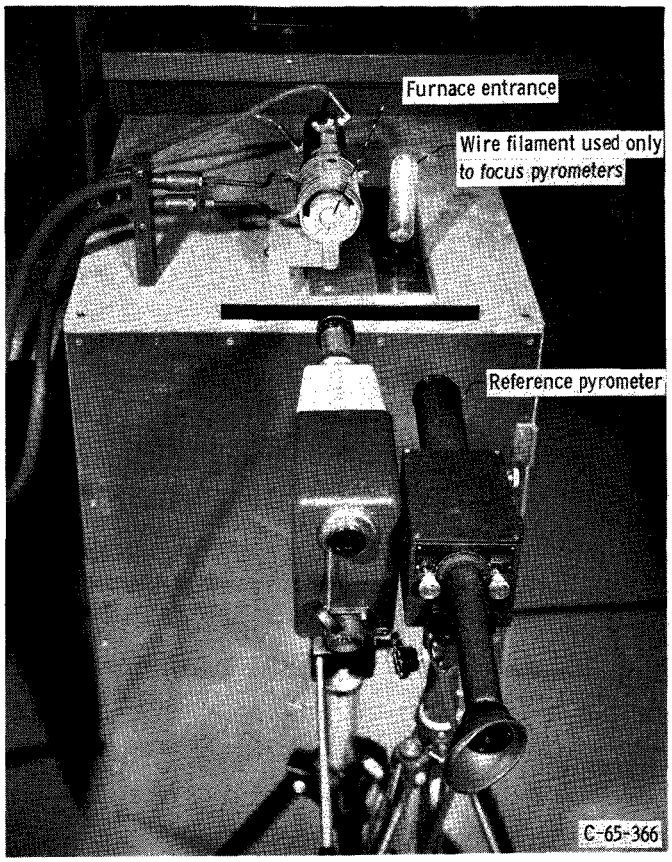

Figure 11. - Graphite furnace.

Visual Optical Pyrometers

Standard-deviation data gathered from national standards laboratories throughout the world by the NBS (ref. 3) are shown in table II for visual optical pyrometers and for tungsten strip lamps. The NBS reports that these standard-deviation data should be related to the uncertainties stated on certificates of calibration (fig. 8, p. 16), but that insufficient data were available to do so. Instead, preliminary estimates of the type given in table II together with the available data on the stability of strip lamps and pyrometers have been used to make judgment-type estimates of the total error under the assumption that the signs associated

TABLE II. - PRELIMINARY ESTIMATES FOR STANDARD DEVIATIONS OF VARIOUS ERRORS ASSOCIATED WITH OPTICAL PYROMETER AND STRIP-LAMP CALIBRATIONS ON THE INTERNATIONAL PRACTICAL TEMPERATURE SCALE (REF. 3)

Type	Strip lamp		Pyrometer	
	1063° C	2300° C	1063° C	2300° C
	Error, °C			
[a]Random: s(e)	0.3	0.9	0.3	1.4
[b]Systematic:				
s(a)	0.5	0.8	0.5	1.8
s(b)	.3	.6	.3	1.4
s(c)	<.5	<2.0	<.5	<2.0

[a]From set of observations by single observer.
[b]Associated with observers, s(a); apparatus, s(b); and national standards laboratory, s(c).

with the several errors are the same. These are called maximum uncertainties on the calibration certificates such as that shown in figure 8 (p. 16).

At present visual-optical-pyrometer design has as its principal limitation the precision and accuracy of the observer (refs. 3 and 9). Nevertheless, the accuracy of realizing the IPTS, even with visual pyrometry is now better than the agreement of the IPTS with the TTS (compare fig. 2, p. 3 and table II). A revision of the IPTS will be desirable as soon as the exact magnitude of the disagreement is known (ref. 1, p. 487).

What has been described thus far is the work of national standards laboratories. Uncertainties in temperature values obtained with commercially available visual optical pyrometers calibrated by means of secondary standards can be no better than the uncertainty values of figure 8. Stability of visual optical pyrometers was discussed in the section PYROMETER CALIBRATION.

Photoelectric-Optical and Two-Color Pyrometers

In the case of automatic pyrometers (those providing a direct temperature reading or record), the physical complexity of the instrument is much greater than it is in the case of the visual optical pyrometer. Hence, instability, that is, long-term drift error, is of major importance. A discussion of this error is provided in reference 2 (p. 840): "Estimates of probable long term parameter uncertainties involve a combination of experience, experimental data, and engineering judgment. The drift terms should be summed on a statistical basis in accordance with their randomness and independence. . . . It is assumed that the instruments are designed, constructed, and applied in accordance with the best engineering practices known at this time." Some specific requirements are

(1) Effective measures have been taken to minimize the influence of detector sensi-

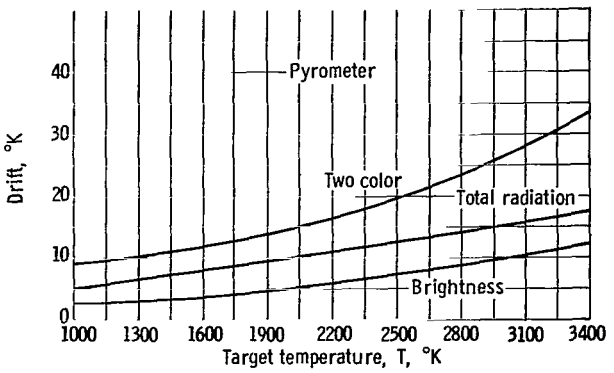

Figure 12. - Estimated long-term drift errors of automatic pyrometers (ref. 2, p. 841).

tivity; e. g., by the use of very stable reference sources and scanning techniques, unless the detector is inherently stable in the order of 0. 5 percent.

(2) Great care is exercised to protect the optics of the instrument from environmental and internal sources of contamination.

(3) The most stable optical components and materials available are used. Narrow-band and spectral-compensating filters are used in the manner required to minimize spectral and other drift errors.

(4) Electronics and electromechanical elements are highly stabilized.

"Figure 12 is a plot of the estimated probable long-term instability of automatic radiometric pyrometers . . . . Certain design approaches, other than those assumed here, would result in difference errors due to effective wavelength uncertainty, but such differences will not seriously affect the end results." The source of each of several errors contained in each curve of figure 12 are described in reference 2 (p. 840). While these long-term errors may be somewhat reduced by calibrating at necessary intervals of time, it is obvious that drift is a serious detriment to accuracy, particularly for ratio instruments. Also, since automatic pyrometers are calibrated directly or indirectly by means of visual optical pyrometers, uncertainties in the accuracy of the calibration standard must be added to the error data of figure 12. Data for total radiation pyrometers were included in figure 12 to show the status of this type of instrument. In general, total-radiation pyrometers are very sensitive to the variation of spectral emittance with wavelength and also require relatively large targets.

Precision, on a short-time basis, is quite another story. Many automatic instruments can sense temperature changes so small that they are undetectable by the human eye. As mentioned earlier, photoelectric optical pyrometers have the potential of improving optical pyrometry accuracy tenfold; however, the task of accomplishing this improvement by using automatic methods is very great.

MINIMIZATION OF ERROR DUE TO SMALL OR AWKWARDLY LOCATED SOURCE

Pyrometers yield erroneous temperatures when sighted on sources that are too small. Also, errors occur when a piece of hardware obstructs a portion of the light

rays directed from the source to the target. By discussing the last problem first, several of the expressions pertinent to the small-target problem can be illuminated.

Vignetting

Vignetting, or ray blocking, arises from nonuniform radiance of the source at the image plane, which in the case of a visual optical pyrometer is the plane of the filament. The operator can frequently detect the existence of a pronounced case of vignetting by his inability to obtain filament disappearance. For photoelectric pyrometers, no such warning exists. In the following example, sightings are being made on the bottom of a cylindrical cavity (fig. 13). The entrance pupil diameter d, which incidentally is governed by the objective aperture, is established by rays m_1 and m_2. This diameter is 1.4 centimeters for a commonly used pyrometer but is only 0.3 centimeter for the human eye. Let the cavity of figure 13 have a diameter D larger than 0.3 centimeter and smaller than 1.4 centimeters. An eye located in place of the objective lens can view the full area of the cavity bottom without obstruction. Now move the eye so that it is sighting through the pyrometer optical assembly. The eye is able to view the full area of the cavity bottom and a large amount of the surrounding area, but the eye's unhindered view of the cavity bottom extends only to the diameter w as defined by rays m_1 and m_2. At a greater value of the diameter w, some rays beamed toward the entrance pupil are blocked by the cylinder walls; therefore, the source does not appear to be of uniform brightness. Furthermore, any other hardware that intercepts the bundle of rays bounded by m_1 and m_2 will cause the source w to appear to be of nonuniform brightness.

If w happens to be the minimum permissible target diameter for zero pyrometer error, the minimum cavity diameter D required to eliminate vignetting is determined from geometry (fig. 13) to be

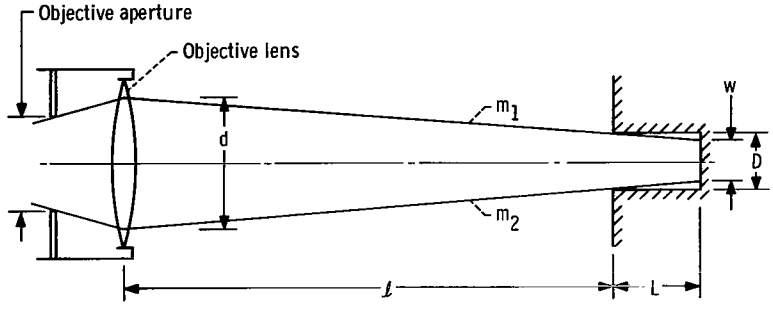

Figure 13. - Schematic diagram of pyrometer focused on back wall of cavity. Diameter of cavity entrance, D; entrance pupil diameter, d; depth of cavity, L; distance, ℓ; rays, m_1 and m_2; target diameter, w.

$$\frac{D - w}{L} = \frac{d - D}{\ell} \tag{22}$$

For some pyrometers, the entrance pupil is smaller than the value used in the example. In such instances, the vignetting problem is less important, but must not be neglected if maximum accuracy is desired. Because vignetting affects both bands in a similar manner, ratio pyrometers are less sensitive to vignetting than are optical pyrometers.

Minimum Error-Free Target Size

Many modern pyrometer types are capable of accurately sensing the temperature of small targets. In the following discussion on the size of these small targets, the target area itself is presumed to be uniformly bright. For photoelectric optical pyrometers (fig. 6, p. 11), the field stop located at a focal plane defines the size of the source as seen through the ocular. Only the center area (target) of this image, usually denoted by a circular reticle in the ocular, is imaged on the photomultiplier tube. Obviously, the target area must completely fill the aperture of the photomultiplier tube. For temperatures above 1000° C and for a filter band pass of 300 angstroms at 6500 angstroms, automatic brightness pyrometers with a target diameter as small as 0.025 centimeter at a distance of 25 centimeters are commercially available. Since most pyrometers are distance compensated, the size of the source being sensed increases in direct proportion to the distance between the pyrometer and the source.

One ratio pyrometer available on the market requires a slightly larger source than does a photoelectric optical pyrometer of comparable quality; however, minimum target size varies more with manufacturer than it does with pyrometer type.

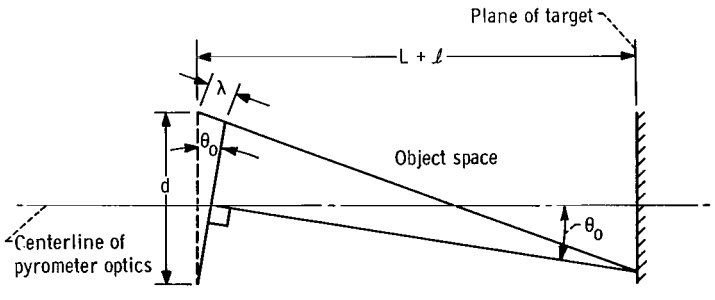

Figure 14. - Diagram showing construction of theoretical image resolution angle. Entrance pupil diameter, d; depth of cavity, L; distance, ℓ; wavelength, λ; theoretical angular resolution, θ_0.

An observer using a visual optical (disappearing filament) pyrometer usually views an area much larger than the particular source he is attempting to measure. There is no reticle or other built-in device that defines the minimum error-free target size. The minimum target-size problem has been examined by D. R. Buchele of Lewis and his findings are contained herein. Situations examined are those in which the

Pyrometer	Entrance pupil diameter, d, cm	Theoretical image resolution angle, θ_o, rad
A	0.445	0.000146
B	1.420	.000046

target has greater brightness than the surrounding area. This presentation shows how the minimum error-free target diameter of a good quality disappearing-filament pyrometer can be determined.

The theoretical image resolution angle θ_o is approximately equal to λ/d, where λ is the wavelength of the light, and d is the entrance pupil diameter (ref. 15). For example, at 6500 angstroms the resolution of the human eye θ_o is $6500\times10^{-8}/0.3$ radian or 3/4 minute of arc. Figure 14 shows how θ_o of a pyrometer is related to the region of object space, also called the angular field of the pyrometer. The angular resolution of two typical disappearing-filament pyrometers at 6500 angstroms is shown in the preceding table.

The field angle subtended by the filament diameter referred to object space θ_f is readily obtained from the measurement of the apparent filament diameter d_f for a given distance $\ell + L$ between the pyrometer objective lens and the target. Using,

$$\theta_f = \frac{d_f}{\ell + L} \simeq \frac{d_f}{\ell}$$

Pyrometer	Field angle subtended by filament diameter θ_f, rad	Relative filament size, θ_f/θ_o
A	0.0008	5.5
B	.00014	3.0

gave the field-angle data for the two pyrometers shown in the table at the left. The last column shows the relative size of the filament to the minimum theoretical image length. This is a constant of the pyrometer. Relative to its resolving ability, the filament of A is larger than that of B.

From experiments involving pyrometer A, Buchele drew several conclusions. The minimal size target that requires no correction is a square that has a width 10 times the theoretical optical resolution of the pyrometer; hence, $\theta_t/\theta_o = 10$. Even smaller targets exhibit zero error provided the temperature of the surrounding area is near the target temperature. However, at a value of $\theta_t/\theta_o = 5$, 1-percent errors arise when the target temperature and the surrounding-area temperature differ by as little as 100° C. A circular target required values of θ_t/θ_o about 50 percent greater than the values of θ_t/θ_o observed for square targets.

The link between different pyrometers is the ratio θ_t/θ_o. If this ratio has the same value for all pyrometers of comparable optical quality, the minimum error-free target diameter of another pyrometer is readily determined because

$$w = \frac{\theta_t}{\theta_o}\theta_o\ell = \frac{15\lambda\ell}{d} \tag{23}$$

The results for circular sources are presented in the following table:

Pyrometer	Theoretical angular resolution, θ_o	Relative filament size, θ_f/θ_o	Relative target size, θ_t/θ_o	θ_t/θ_f	Target diameter distance (at ℓ = 25 cm), w, cm
A	0.000146	5.5	15	2.73	0.051
B	.000046	3.0	15	5.00	.017

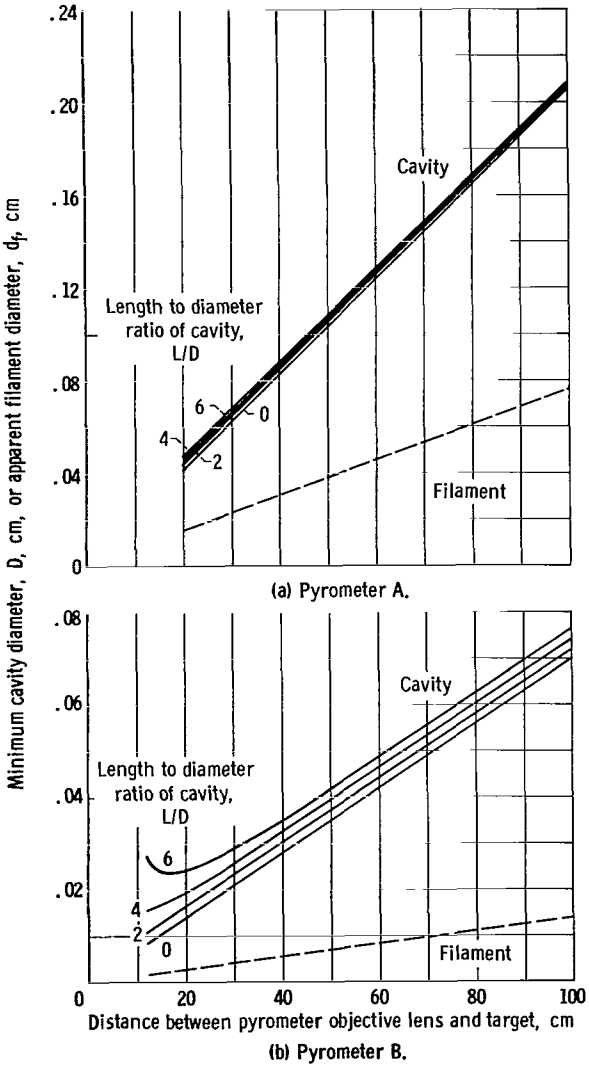

Figure 15. - Minimum cavity diameter for error-free observation of bottom of cylindrical cavity. Disappearing-filament pyrometer alined along axis of cavity. (Minimum error-free target diameter corresponds to curve of L/D = 0.)

The validity of equation (23) for the pyrometer B has been confirmed to the extent that no corrections were required at a diameter w of $15\lambda\ell/d$. Filament size and minimum error-free target diameter w are shown in figure 15 for both pyrometers. The target is assumed to be of greater brightness than the surrounding area. If the target diameter is reduced 50 percent, a temperature error can be anticipated. Included in figure 15 are values of minimum cavity-entrance diameter D necessary to eliminate vignetting error due to rays being blocked by the cylindrical walls (see eq. (22)).

CAVITY EMITTANCE

The Blackbody

Temperature determinations were shown previously in this report to be of the best accuracy when the source was a blackbody. For this case, emittance is 1 and reflectance is zero; correction equations (9) and (13) are superfluous because S_B (or S_C, as the case may be) equals T; width of the filter band pass and the value of the effective wavelength are of small

concern. However, the principal advantages of blackbody sources are to be found elsewhere. Energy incident on a blackbody cannot be reflected into the field of the pyrometer and therefore an erroneous temperature reading results. Also, uncertainties in the value of T due to uncertainty in the value of emittance are eliminated whenever blackbody sources are used (eqs. (14) and (15)).

A truly black surface capable of being viewed by a pyrometer does not exist. One method of obtaining pyrometer targets of large and well-defined values of emittance is the use of a cavity in the emitting surface.

Cavity Design Considerations

Surfaces that have low emittances are common. The emittance can be increased greatly and even made to approach 1 by letting the surfaces "see" themselves. This can be accomplished by deep roughening of the surface, or better still, by drilling a cavity. Figure 30 (pp. 56 to 61) can be used to explore the pronounced difference in the brightness temperature of a surface (typified by an emittance of 0.4) compared with a cavity (typified by an emittance of 0.96). For spectral radiation, absorptance equals emittance, and both are equal to 1 minus the reflectance:

$$\alpha = \epsilon = 1 - \rho \tag{24}$$

Hence, the low-emittance surface cited reflects 60 percent of energy incident upon it compared with only 4 percent reflected by the cavity. In this example, the quantity of stray radiation that could enter a pyrometer is reduced fifteenfold by replacing the low-emittance surface with a cavity.

The emittance of a cavity is defined similarly to that of a surface. The issuing flux, which includes both emitted and reflected components, comes from an area of interior wall opposite the opening. The reflected component is a result of radiation from the remainder of the cavity that is incident on the measured area.

A cavity requires several features to be a desirable target on which to sight a pyrometer.

(1) The target diameter w should be at least equal to the minimum error-free target size.

(2) The emittance should be as near 1 as practical.

(3) The radiance over the target area should be uniform.

(4) The walls should be as nearly isothermal as possible.

(5) The emittance should not change with time.

(6) The cavity should be reproducible in manufacture.

The aforementioned items are in many ways interrelated. Insofar as possible, they are discussed in order.

The minimum cavity diameter, item (1), is determined primarily by the pyrometer optics and the pyrometer-to-target distance. Cavities smaller than 0.02 centimeter in diameter have been shown to be sufficiently large under some circumstances (e.g., fig. 15).

Items (2) and (3) require further clarification. A flat surface that radiates diffusely has an emittance that is independent of the angle of view. Just as a flat surface does not necessarily radiate in a diffuse manner neither is a cavity expected to do so. In fact, the surfaces of most materials are not diffuse radiators. In turn, they do not reflect incident light in a diffuse manner; that is, some of the light is preferentially reflected in a specular (mirror-like) manner. (The subject of diffuse and specular radiation is treated in most radiant-heat-transfer texts.) Cavities used as pyrometer targets are usually viewed along the cavity axis. Consequently, cavity emittance other than along the axis need not be of concern. However, the nondiffuse behavior of the local cavity surfaces themselves can play a significant role in determining the magnitude of the cavity emittance as measured along the cavity axis. Thus far, this discussion has presumed that a given cavity has only one emittance ϵ_c, that is, the target area is considered to be uniformly bright. When nonuniform brightness is of concern, a local cavity emittance ϵ_a will be used to denote the emittance at a particular location within the cavity.

Numerous analytical methods for evaluating the emittance of cavities are available in the literature. Kelly and Moore (ref. 12, p. 117) and also DeVos (ref. 16) have described three general methods that have been employed to derive cavity-emittance equations. These three methods are described briefly, and analytical results for cylindrical cavities are compared.

The DeVos method of evaluating ϵ_c is based on a calculation of the influence of the

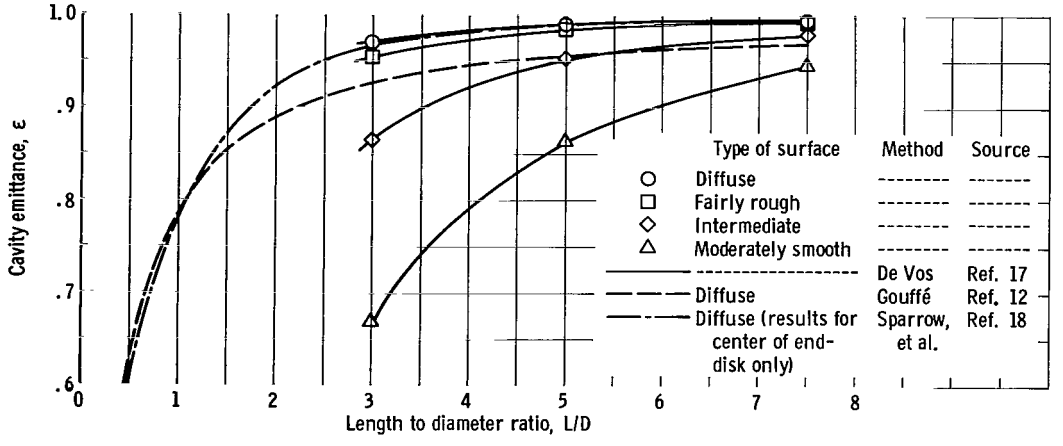

Figure 16. - Results of three different analytical methods for evaluating emittance of cylindrical cavity. Surface emittance, 0.4; isothermal walls.

cavity on the radiation from other surface elements. These surface elements can be made to reflect and hence to emit in a directionally selective manner. The derived expression cannot be easily applied, particularly to shallow cavities. To the author's knowledge, evaluations have been made only at a wall emittance value of 0.4. Emittance results computed by Edwards (ref. 17), who used the DeVos method (ref. 16), are shown in figure 16 for cylindrical cavities whose walls possess an emittance of 0.4. Substantially larger values of ϵ_c are obtained with perfectly diffuse walls than with moderately smooth walls typical of smooth, clean, metal surfaces. Diagrams for the directional emittance distribution of the surfaces associated with curves for fairly rough, intermediate, and moderately smooth curves are shown in both references 16 and 17. Little encouragement can be offered on how to determine the specularness of a surface other than to conduct reflectance measurements. Generally, the rougher and more porous a surface becomes, the nearer it comes to being an ideal diffuser and also to being a blackbody.

The second method develops the emittance expression by considering the flux coming from a surface element opposite the opening. This flux includes not only that emitted by the element, but also that reflected by the element from other areas of the enclosure. This method, as used by Sparrow, Albers, and Eckert (ref. 18), is particularly noteworthy in that it is possible from their analysis to obtain an evaluation of the local cavity emittance ϵ_a of any elemental area on the walls of a cylindrical enclosure. A rigorous evaluation applies only to a perfect diffuser. The data of reference 18 have been extended to a wide range of surface emittance values and are presented in table III and figure 17.

The third method, used by Gouffé, is described in detail in references 10 (p. 515) and 12 (p. 117) and was proposed therein for use with shallow cavities. It is similar to the second method in that it can be rigorously applied only to perfect diffusers. Mathematically, the expression is relatively simple and easily lends itself to other geometric shapes. Gouffé's results for cylindrical cavities are presented in figure 18.

The results of the three analytical methods are compared in figure 16 for diffuse surfaces. Because it has been shown that (1) the Gouffé equation appears suited only for small values of L/D, (2) the DeVos equation is for deeper cavities, and (3) the Sparrow, et al., equation is suited to both deep and shallow cavities, it is pleasing to find that the ϵ_a values of Sparrow, et al., closely fit the ϵ_c values of Gouffé and of DeVos in those regions where agreement is expected. The Sparrow, et al., results (fig. 16), which are really ϵ_a values obtained at the center of the end-disk, are about 1.1 percent lower than ϵ_a values obtained at a value of r/R of 0.5 for a cavity L/D ratio of 1 (table III); hence, a relatively large diameter cavity would be required in order to obtain a central area of reasonably uniform emittance. This observation is damaging to arguments on behalf of small values of L/D when a minimum depth of cavity is desired.

Deep cavities can conflict with item (4), the desirability that the cavity walls be nearly isothermal. The analysis presented to here has recognized only isothermal

TABLE III. - APPARENT EMITTANCE[a] OF END-DISK OF CYLINDRICAL CAVITY

Length to diameter ratio, L/D	Fractional distance from disk center to periphery, r/R	Surface emittance, ϵ							
		0.9	0.75	0.5	0.4	0.3	0.2	0.1	0.05
		Apparent emittance, ϵ_a							
1/2	0	0.9480	0.862	0.6878	0.6004	0.4975	0.3724	0.2136	0.1156
	.5	.9545	.878	.7130	.6278	.5250	.3967	.2299	.1251
	.8	.9634	.899	.7523	.6710	.5689	.4363	.2568	.1409
	1.0	.9708	.918	.7891	.7130	.6132	.4778	.2862	.1585
1	0	.9782	.938	.8395	.7785	.6950	.5728	.3756	.2227
	.5	.9800	.943	.8489	.7898	.7077	.5857	.3859	.2294
	.8	.9824	.950	.8632	.8072	.7276	.6063	.4026	.2403
	1.0	.9848	.955	.8793	.8273	.7510	.6310	.4231	.2540
2	0	.9938	.981	.9461	.9197	.8768	.7983	.6232	.4297
	.5	.9940	.982	.9479	.9222	.8802	.8027	.6279	.4335
	.8	.9942	.983	.9506	.9262	.8856	.8096	.6356	.4398
	1.0	.9946	.985	.9561	.9333	.8948	.8208	.6474	.4493
3	0	------	.9919	.9768	.9650	.9439	.8994	.7751	.5974
	.5	------	.9920	.9773	.9657	.9450	.9010	.7774	.5997
	.8	------	.9922	.9780	.9668	.9466	.9036	.7811	.6035
	1.0	------	.9938	.9815	.9712	.9522	.9105	.7893	.6111
4	0	.9984	.9956	.9880	.9822	.9714	.9465	.8638	.7189
	.5	.9984	.9956	.9882	.9824	.9718	.9472	.8649	.7204
	.8	.9984	.9957	.9884	.9827	.9723	.9482	.8668	.7227
	1.0	.9988	.9971	.9914	.9864	.9768	.9536	.8718	.7292
5	0	------	------	.9929	.9897	.9838	.9697	.9158	.8051
	.5	------	------	.9930	.9898	.9839	.9700	.9164	.8060
	.8	------	------	.9930	.9899	.9841	.9703	.9173	.8074
	1.0	------	------	.9959	.9934	.9883	.9753	.9232	.8135
6	0	------	.9981	.9954	.9934	.9900	.9817	.9468	.8656
	.5	------	.9981	.9954	.9935	.9901	.9818	.9471	.8661
	.8	------	.9981	.9954	.9935	.9901	.9819	.9475	.8670
	1.0	------	.9995	.9982	.9969	.9942	.9867	.9531	.8728
8	0	------	------	.9976	.9967	.9953	.9920	.9766	.9320
	.5	------	------	.9976	.9967	.9953	.9920	.9767	.9322
	.8	------	------	.9976	.9967	.9953	.9920	.9768	.9325
	1.0	------	------	1.0004	1.0002	.9994	.9967	.9822	.9382
10	0	------	------	.9985	.9980	.9973	.9958	.9889	.9635
	.5	------	------	.9985	.9980	.9973	.9958	.9888	.9636
	.8	------	------	.9985	.9980	.9973	.9958	.9889	.9637
	1.0	------	------	1.0013	1.0014	1.0013	1.0005	.9943	.9694
14	0	------	------	.9993	.9990	.9988	.9983	.9962	.9880
	.5	------	------	.9992	.9990	.9987	.9982	.9962	.9880
	.8	------	------	.9993	.9991	.9988	.9983	.9963	.9881
	1.0	------	------	1.0008	1.0010	1.0015	1.0023	1.0017	.9939

[a]Calculated by the method of Sparrow, et al., ref. 18.

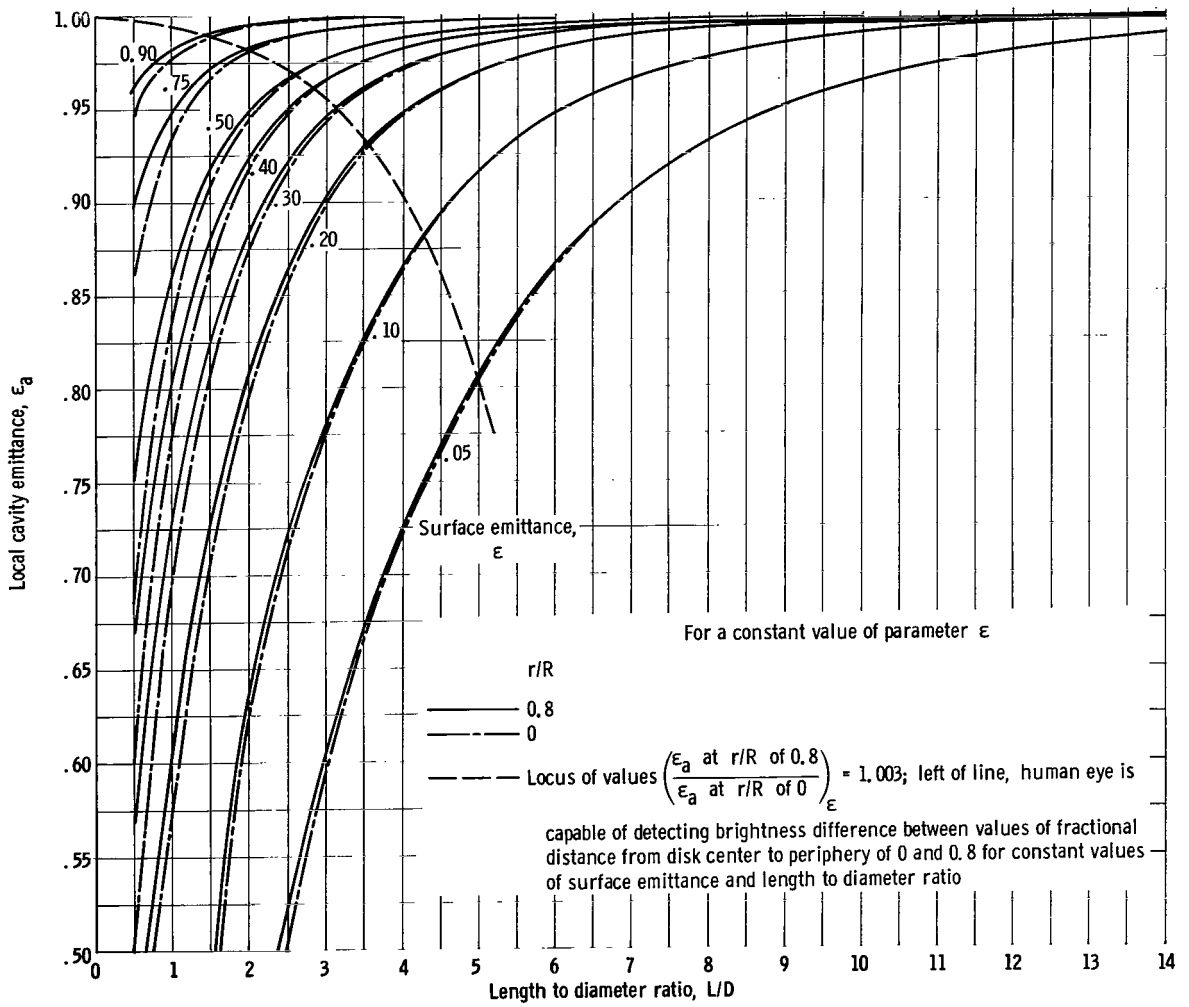

Figure 17. - Emittance of circular disk enclosing end of cylindrical cavity. At each value of surface emittance, lines are shown for two values of fractional distance from disk center to periphery (ref. 18).

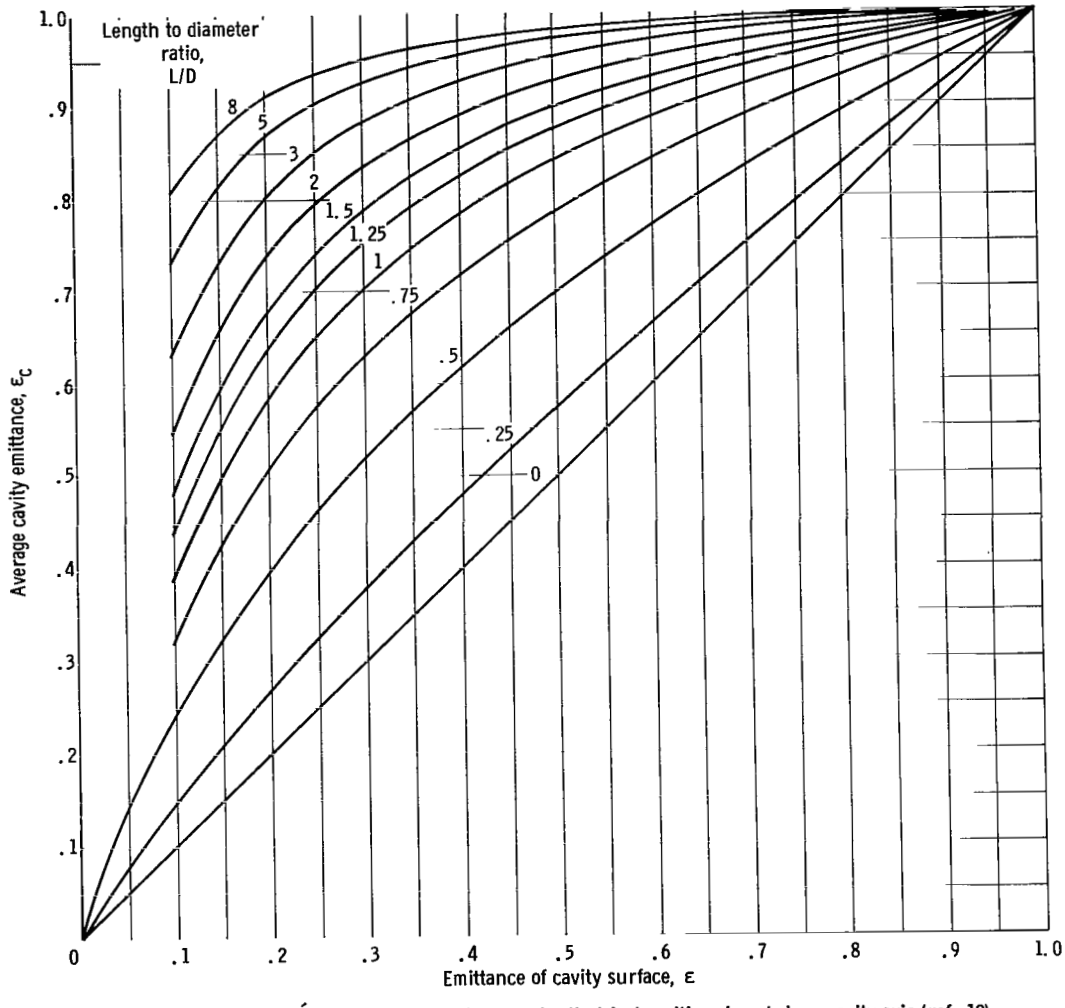

Figure 18. - Gouffé expression for emittance of cylindrical cavities viewed along cavity axis (ref. 12).

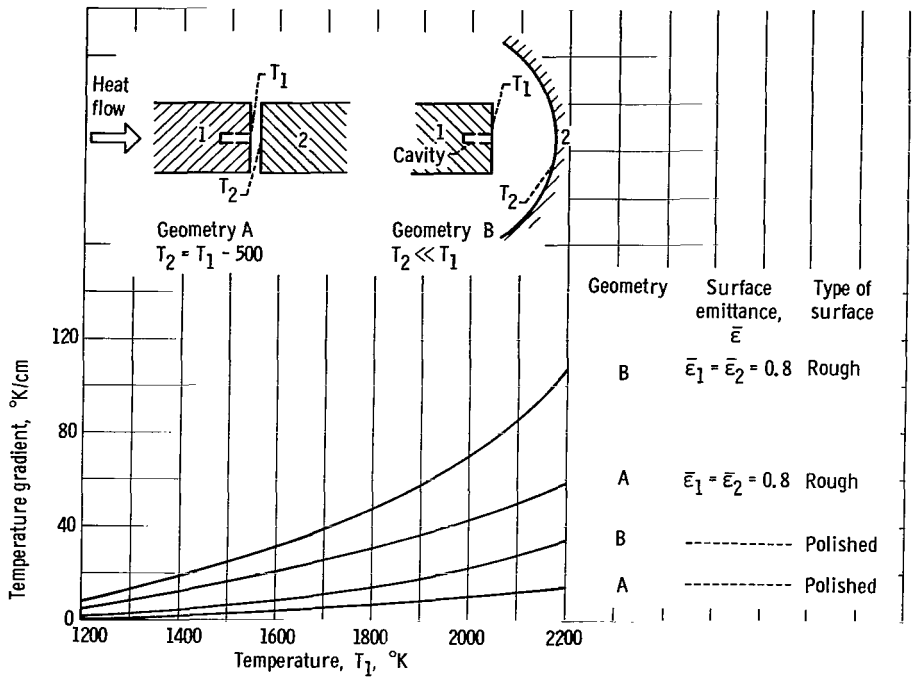

Figure 19. - Temperature gradient in tungsten bar subject to unidirectional heat flow normal to exposed surface. Heat removal entirely by radiation.

cavities; however, refractory materials, ceramics and metals alike, are not particularly good conductors of heat. Also, an increase in temperature for many materials (e.g., tungsten) results in a decrease in the value of thermal conductivity. Hence, the interior and the surface of a material can be at considerably different temperatures. In the simple, unidirectional heat flow example of figure 19, temperature gradients in a tungsten bar are presented for several differing environmental conditions. The back wall of a 0.5-centimeter-deep cavity is as much as 35° K hotter than the surface when temperatures are near 2000° K. Temperature nonuniformities of this magnitude can introduce sizeable error in surface temperature determinations.

The stability of cavity emittance with time, item (5), presents several problems. The desirability of a roughened cavity surface has been stressed. Oxidation, evaporation, lattice distortion, crystal reorientation and growth, and surface migration can drastically alter emittance characteristics of the initially fabricated surface. The extent of surface change can be highly dependent on the material, fabrication technique, and environmental conditions. The cavity material should be extensively aged in a gaseous environment whose composition compares closely with the normal operating environment. While aging can be accelerated by applying operating temperatures that are higher than normal, such an undertaking requires considerable skill.

An infrequent but very obnoxious form of migration within cavities must be guarded against. During the course of one investigation, whisker growth occurred on cavity

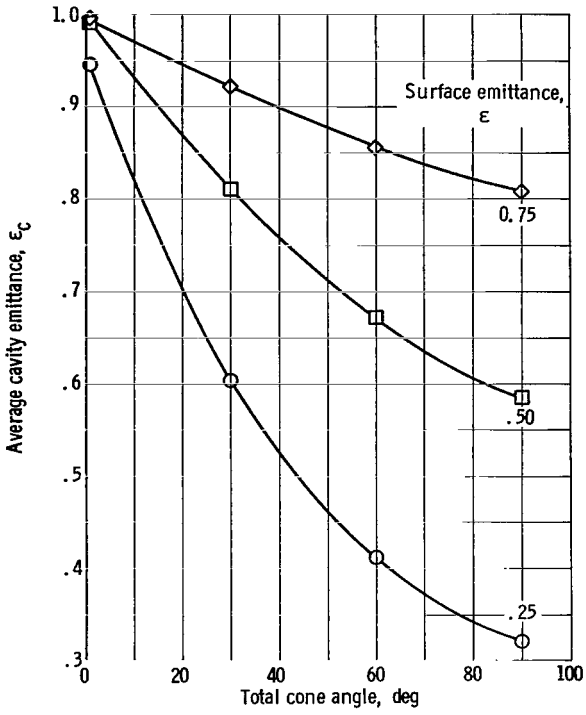

Figure 20. - Emittance of cone when angle made by line of view and cavity axis is less than cone half-angle for diffusely radiating surfaces (ref. 19).

surfaces during the initial heat of a molybdenum bar being tested in vacuum. The growth was rapid, occurred below a temperature of 1400° C, and resulted in a marked lowering of cavity emittance. This latter effect can be attributed to the relatively large surface area of the whiskers, many of which were longer than the cavity diameter. After several hours at 1400° C, the bar was cooled, cleaned by gentle scraping, and returned to the vacuum vessel. On further heating, whiskers did not develop. The observed whisker diameter was only about 0.001 centimeter; hence, this nuisance cannot always be readily detected.

The foregoing discussion on surface stability illustrated one of the difficulties encountered when good cavity reproducibility, item (6), is desired. Also, cavities must conform reasonably well to a simple geometric shape when a direct comparison of analytical and experimental values of ϵ_c is desired. For small cavities, cylinders and cones are logical choices. In general, acceptably shaped cones are more difficult to reproduce than their cylindrical counterparts. Some rounding of the cone apex is unavoidable. Apex rounding aggravates brightness nonuniformity at the target center and makes measurement of cone angle difficult. Influence of cone angle on ϵ_c is shown in figure 20 (ref. 19) for diffuse radiators.

Cone emittance increases as the surface becomes more specular (ref. 17). This effect, which is opposite the emittance behavior of cylinders (fig. 16, p. 29), further illustrates the need for accurately fabricated cavities.

Comparison of Experimental and Analytical Results

Little experimentally obtained ϵ_c data exist in the literature, and all data should be weighed against the precautions that have been cited herein. A method for determining ϵ_c for clean, refractory-type metals is presented in appendix D. Experiments conducted with this apparatus have provided a basis for many of the precautionary remarks of the preceding section. Again, the experimental results that follow serve primarily

to define, rather than answer, the problems one encounters in the selection of a cavity to be used as a pyrometer target.

Diffusely radiating surfaces. - Experimentally obtained values of emittance for shallow cylindrical cavities with diffusely radiating surfaces are compared to several theoretically derived emittance expressions in reference 12 (p. 117). The L/D ranged from 0.25 to 1, the line of view was close to the axis, and the viewed area was near the center of the end-disk actually resulting in local cavity emittance ϵ_a measurements. Experimental results were in close agreement with the ϵ_a results of Sparrow, et al., (fig. 17, p. 32) and the ϵ_c results of Gouffé (fig. 18, p. 33). For L/D values greater than 3, the theoretical results of Sparrow, et al., and DeVos are in good agreement (fig. 16, p. 29). Analytically, both methods appear more rigorous than that of Gouffé.

The results of the method of Sparrow, et al., are to be recommended for cylindrical cavities with diffusely radiating walls. Although unsubstantiated by experiment, the values in figure 20 (ref. 19) appear sound for cones whose internal surfaces are perfect diffusers.

Nondiffuse surfaces. - The apparatus, fabrication technique, and computational procedure discussed in appendix D were employed to study cavities in tungsten and molybdenum. The optical pyrometer had optical characteristics shown in figure 15(b) (p. 27). Cavities 0.025 to 0.14 centimeter in diameter were drilled by an electrical-disintegration method. This process roughened the cavity surfaces by pocking them to a depth of about 0.001 centimeter. Under the microscope, all surfaces appeared to be of the same roughness. Outgassing, cleaning, and aging were carried out in a vacuum environment of 10^{-6} torr or lower. Only after the molybdenum was aged a day at 2000° K did the cavity emittance values appear independent of time. (This operation was performed after the whiskers, mentioned previously, had been eliminated.) It must be noted that a month-long exposure to room atmosphere necessitated repeating the aging treatment. Tungsten surfaces appeared less sensitive to environmental conditions. Tungsten aging was conducted at about 2350° K for 1 day, which was likely insufficient to anneal the material completely; however, changes of tungsten ϵ_c values with time were not observed for the considerable number of hours required to obtain the data presented herein.

After aging, the pocks on both metals remained, but the local surfaces took on a sheen. The aged surfaces themselves had emittances of near 0.5 and 0.4 for tungsten and molybdenum, respectively; these measurements were taken on an originally flat surface that had been roughened by the electrical-disintegration drill to simulate the internal-surface roughness. The cavity emittance results are not readily compared with the theoretical results presented earlier. For example, the tungsten curve (fig. 21) lays much lower than the curve from Sparrow, et al. (fig. 17) at an r/R of zero and wall emittance of 0.5.

The variation of ϵ_a with r/R was observed to be greater than that shown in

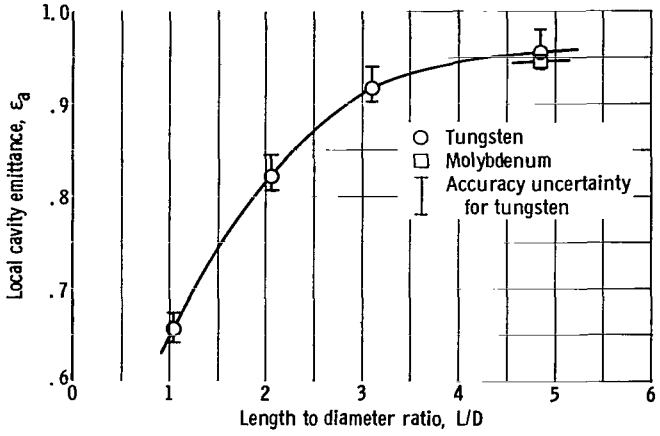

Figure 21. - Experimentally determined emittance. Cylindrical cavities drilled by electrical-disintegration method. Measurements made on center of end-disk. Temperature range, 1500° to 2200° K.

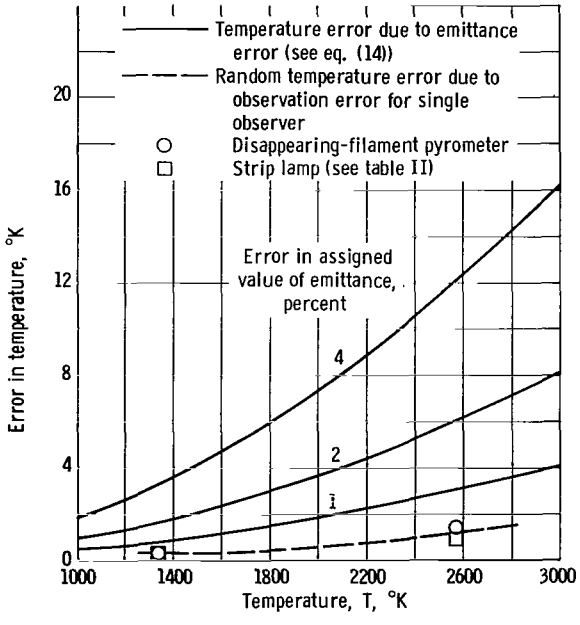

Figure 22. - Comparison of temperature errors arising from variation in emittance and from sensitiveness of the human eye.

figure 17. In fact, the L/D had to be 3 for tungsten and 5 for molybdenum before the end-disk exhibited a reasonably uniform brightness over the center two-thirds of the area. (The dashed line that cuts across the emittance curves of fig. 17 denotes the minimum spread between the curves for r/R of 0 and 0.8 that is detectable by the human eye. This line was obtained with the aid of fig. 22.)

The aforementioned observations, judged on the basis of figure 16, indicate that both molybdenum and tungsten definitely do not behave as ideal diffusers. The curve for an intermediate surface (fig. 16), if adjusted to an emittance of 0.5, would probably provide a reasonably good fit to the tungsten data (fig. 21).

The emittance behavior of a backwall of nonuniform brightness is illustrated in figure 23 for tungsten. These data were obtained by two observers at three values of pyrometer-to-target distance. The cavity diameter was about 0.1 centimeter. Each observer made four measurements at each position shown. The pyrometer was always focused on the center of the end-disk. Values of ϵ_a obtained at a distance of 45 centimeters are the same as those shown in figure 21. At this relatively close distance, the size of the end-disk is large compared with the filament diameter, and hence, a brightness temperature match can be obtained for a local area very close to the center of the end-disk.

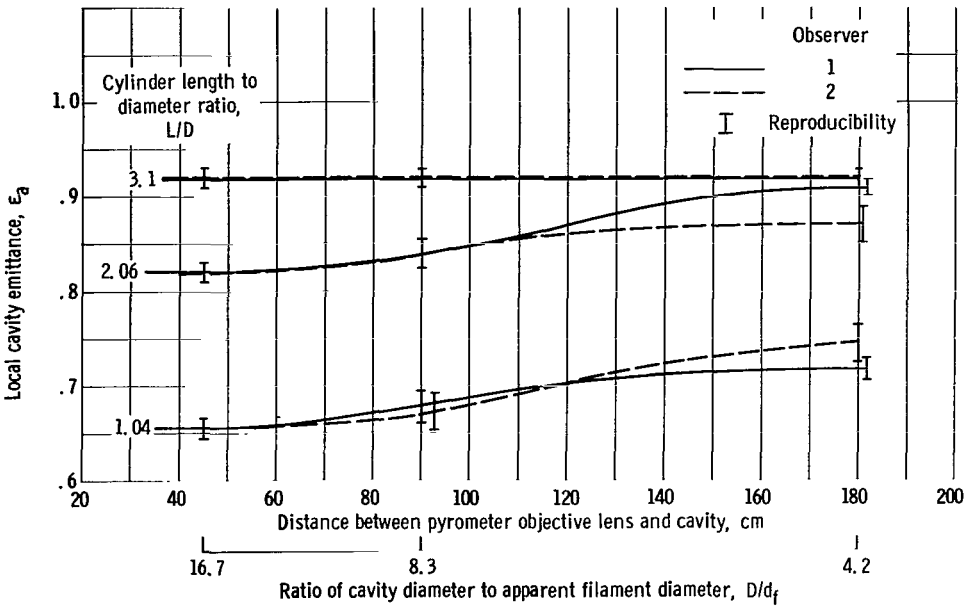

Figure 23. - Nonuniformity of emittance observed on end-disk of cylindrical tungsten cavity. Pyrometer filament alined on center of end-disk. Cavity fabricated by electrical disintegration technique. , , Temperature, 2200° K.

However, as D/d_f increases (fig. 23), brightness matching requires the use of a larger fraction of the disk area. For shallow cavities, the eye can perceive the brightness to increase markedly as r/R increases. Often, a true brightness match is not possible. At these undesirable conditions, the two observers experienced difficulty in obtaining reproducible measurements (see fig. 23).

Incidently, at a value of D/d_f of 4.2 (fig. 23), the cavity diameter is somewhat smaller than the recommended minimum diameter (fig. 15(b), p. 27). Yet the results shown in figure 23 indicate reproducibility and accuracy (invariance of ϵ_a with D/d_f) for the deepest cavity remain unchanged as D/d_f ranged from 16.7 to 4.2. This apparent inconsistency is eliminated by recalling that figure 15 applies when the surrounding area is at a much lower brightness than the target, whereas the data of figure 23 were obtained by using a surrounding area that had, at most, a 180° K lower S_B value than the target. When D/d_f was reduced to a value of 3.0 for a cavity L/D of 3.1, the reproducibility of measurements suffered.

Pyrometer sightings were made also on conical cavities. As expected, on the basis of previous discussion herein, emittance values were much greater than those for perfect diffusers (compare figs. 20 and 24). Also, the experimental cavity emittance changed very gradually with cone angle. At the two larger cone angles shown, small dark spots were observed at the cone apex because of problems encountered in fabricating sharp, pointed apexes. Furthermore, the cones of large angle produced a low-intensity annular surface on the inner periphery of cone.

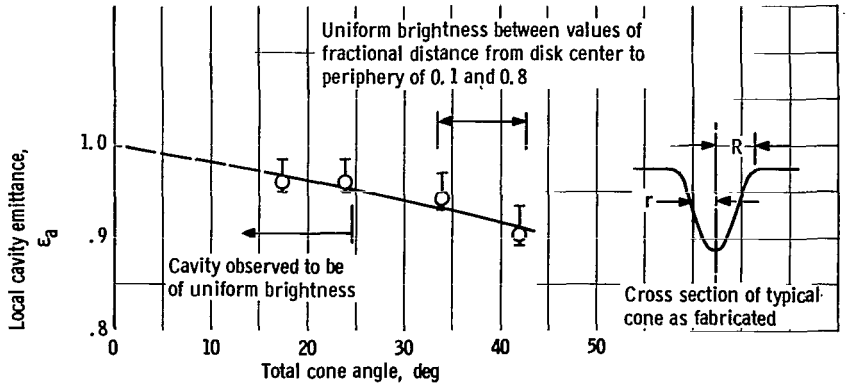

Figure 24. - Experimentally determined emittance of tungsten, conical cavities fabricated by electron-disintegration method. At cone angles less than 30°, measurement was made on apex. For larger angles, measurement was made near apex, but small dark spot at apex was avoided. Vertical bars show inaccuracy in local cavity emittance. Temperature, 1500° to 2200° K.

Summary Remarks

Cavity emittance ϵ_c has been shown to be dependent on many factors not the least of which is the specularness of the cavity surfaces. For other than cavities approaching black, isothermal conditions, direct measurement of ϵ_c is recommended whenever ϵ_c values of good accuracy are desired; however, control of the fabrication process described herein is judged sufficiently good so that the measured emittance of one cavity can be used for another cavity provided that the material and environment are duplicated also.

SURFACE EMITTANCE AND ENERGY TRANSMISSION LOSSES

Thus far this report has treated surface emittance ϵ in a very superficial manner. Likewise, energy transmission losses occurring between the source and the pyrometer have been barely mentioned.

As shown in appendix B, the effective emittance ϵ' equals the product of the source emittance and the transmission of the system, namely,

$$\epsilon' = \epsilon\tau'$$

(For cavities, ϵ is replaced by ϵ_c or ϵ_a.) With ϵ and τ' known, the true temperature can be obtained from equations (C2) and (C3) for optical and ratio pyrometers, respectively. Also, true temperature can be obtained from the conversion charts of

appendix C for certain of the more common values of λ. A guide that may be helpful in obtaining reliable values for ϵ and τ' is presented in the following section.

Surface Emittance

The term surface emittance is somewhat misleading. It is really the bulk material and not the surface that generates the radiant flux emitted at a surface. For many metals, this thickness of bulk material needs to be of the order of 100 atomic diameters for the material to exhibit bulk properties. Some oxide materials, and this includes many high-temperature electrical insulators, are normally classed as being opaque, yet much of the emitted energy originates in a volume extending far from the surface. These materials, being poor conductors of heat, are subject to large temperature gradients. The indicated temperature is an averaged value dependent on the temperature gradients of the volume into which the pyrometer is sighted. The depth of this volume is governed by the absorption coefficient k (see section Energy Transmission Losses).

In the section on CAVITY EMITTANCE, it was stated that considerable knowledge of the material and its history was required in order to define the emittance characteristics of a surface. Stress was given to the import of the specularness of emittance for cavity-type sources. When cavities are not employed, specularness is much less important provided that the pyrometer is sighted somewhere close to the surface normal. Even the most highly polished surfaces exhibit very little variation in directional emittance for directions of up to 40° from surface normal (ref. 20). Hence, normal emittance terminology and data are applicable. Explanation and magnitude of the variation of spectral emissivity with direction are contained in reference 20 for perfectly smooth, ideal materials. Insulators and conductors are shown to behave differently.

An excellent discussion of the effects of surface roughness, surface damage, and surface films on emittance is provided by Bennett (ref. 12, p. 145). Some of his observations are as follows: " . . . solid-state calculations based on band theory yield the emissivity, not the emittance [see appendix A]. The presence of surface damage is measurable, and failure to adequately specify sample condition is largely responsible for wide discrepancies both between theory and experiment and between experiments performed in different laboratories on ostensibly the same materials.

"In the case of a stock material used in engineering, it is frequently not possible to specify accurately the history and condition of the surface, and considerable doubt must therefore exist as to the validity of its calculated emittance.

"The effect of surface roughness on the optical properties of materials was apparently first seriously considered by Lord Rayleigh, who published a paper about it in 1901. The solution, however, has only recently been obtained. If the sizes of the irregularities are of the order of a wavelength or larger, the problem becomes one involving geomet-

rical optics. In this case, the facets of the surface behave like small mirrors pointed in various directions, and the statistical properties of the surface must be known in great detail in order to predict the optical behavior. If, however, the surface irregularities are much smaller than the wavelength, one has a diffraction problem. . . . in the limit, as the surface roughness approaches zero, the emittance clearly assumes the value of that for a perfectly smooth surface." Bennett proceeds, in the region where geometric optics are dominant," . . . surfaces having gross roughnesses such that all values of the slope of the surface irregularities are equally probable might be expected to obey Lambert's cosine law [i. e., perfect diffusers] even though a smooth flat surface of the same material did not." When surface irregularities are smaller than the wavelength of the radiation (diffraction region), Bennett provides evidence showing that the total emitted energy is independent of surface roughness (i. e., total emittance is invariant), but the distribution with direction is affected. (Hence, it is conceivable that a given material could exhibit an emittance of 0. 4 and still conform to each of the several DeVos curves, fig. 16, p. 29, depending on the amount of surface roughness.) Bennett remarks that the concept of invariance in the value of total emittance with surface roughness is contrary to generally accepted beliefs. He states that there is good theoretical evidence, substantiated by experiment, for concluding that, in the diffraction region, an emittance change with roughness change of a material is the result of surface damage introduced in the process of making the surface rough.

Bennett discusses surface damage, introducing the subject by stating "The effect of surface damage and resultant lattice distortion on the optical properties of materials has been grossly underestimated, particularly in the case of metals and of semiconductors at wavelengths shorter than the absorption edge. [i. e., wavelengths of interest in narrow-band pyrometery.] In emission or absorption, the surface layers always act to modify the radiation incident on them from inside or outside of the surface." Bennett remarks that, for these materials, the optical penetration depth is usually smaller than the depth of surface damage, and emission or absorption of radiation actually occurs entirely in the disturbed surface layer. "It has been shown that a minimum amount of surface damage is introduced during sample preparation if etching or electropolishing techniques are used."

Regarding the effects of surface films Bennett states that "Little will be said here about the modification of emittance by surface films. It is worth pointing out, however, that although naturally occurring oxide films may strongly affect the emittance of metals at visible and ultraviolet wavelengths, such films often have relatively little effect in the infrared."

Bennett cites numerous examples to illustrate his discussion. In all cases, it is the visible region rather than the infrared region of wavelength where surface characterization is most pertinent. Reference 12 contains other informative articles relating to the

influence of surface effects on emittance. Little quantitative data exist on the magnitude of these influencing factors. As one might suspect, relative effects usually vary from one material to the next. Several examples are cited, primarily to illustrate the current state of the art.

As shown in reference 12 (p. 165), the reflectance of a steel specimen at 6500 angstroms increased nearly 50 percent when the machine lapping compound was changed from 60-micron diamond to fine aluminum oxide. A clean molybdenum surface that is rough cut (60 μ) yields an emittance 8 percent higher at 6500 angstroms than a polished surface (ref. 21), yet for clean tantalum surfaces the same reference showed that a 120-micron cut surface had an emittance value little different from that of a polished surface. Another example (ref. 22) shows the effect of various ordinary finishing processes on the radiation characteristics of aluminum, titantium, and 303 stainless steel. Lapping, honing, grinding, sanding, and metal cutting are shown therein to increase the emittance as much as 0.2. The emittance changes were not particularly wavelength selective. The authors, Edwards and Catton, thought the mechanism to be one of surface deformation that changed the surface properties. On the other hand, they found that sandblasting with micron-size particles increased emittance over 0.5 and showed a pronounced wavelength selective effect. Other mechanisms besides surface damage were attributed to sandblasting. Contrary to what one might expect, rough metal surfaces had directional emittance that increased with off-normal angle more rapidly than did those of smooth surfaces with the same normal emittance.

An oxide-free and degassed refractory-metal surface generally possesses a lower emittance than that evidenced on the first heating cycle. Prolonged heating produces crystal rearrangement and surface migration. Examples were noted in the CAVITY EMITTANCE section of this report. References 21 and 23 show that molybdenum emittance stabilized after an initial heating cycle that ranged up to 1800° K. Higher temperatures are required for tungsten and tantalum. Tantalum gathers oxygen readily even from trace oxygen impurities (0.005 percent) in argon, an inert gas often used to reduce metal evaporation at elevated temperatures (ref. 21). This particular oxidized tantalum surface produced an appreciably higher emittance than clean tantalum.

Sources of Emittance Data

During the past 10 years, numerous compilations of thermal radiative properties of materials have been published. Most textbook tables are of little aid in narrow-band pyrometry because total rather than spectral properties are presented. Spectral-properties data that do exist in collected form are frequently provided at only 6500 angstroms; however, the sources cited herein contain considerable data at visible and near-infrared wavelengths. In some cases, these spectral data are given as reflectance ρ

or absorptance α, either of which can be converted to emittance by the equality

$$\epsilon = \alpha = 1 - \rho \tag{24}$$

which is valid for all opaque materials.

A book by Gubareff, Janssen, and Torborg (ref. 24) provides a widely used review of the literature up to 1959 and contains nearly 300 pages of tables and graphs of spectral emittance and reflectance data for elements, metal alloys and their oxides, and nonmetallic materials. The Data Book (ref. 25) published by the Thermophysical Properties Research Center (TPRC) contains spectral emittance data largely in the form of graphs showing emittance against wavelength for metallic elements and their compounds (ref. 25, vol. 1, ch. 3) and for nonmetallic elements, compounds, and mixtures (ref. 25, vol. 3, ch. 3). The Data Book is based on a world literature survey of articles published since 1940. It is in loose-leaf form to provide for periodic updating. A five-volume compendium, Thermophysical Properties of Solid Materials (ref. 26), includes radiative properties data to 1957. This compendium is being revised and updated (ref. 27) by the Thermophysical Properties Research Center and should be completed by July 1966. The Defense Metals Information Center (DMIC) (Battelle Memorial Institute, Columbus, Ohio) has been publishing a series of memorandums in the general field of radiant heat transfer to help keep the Thermophysical Properties of Solid Materials compendium up to date and more readily available. Specific memorandums on emittance values of selected metals are available. The Electronic Properties Information Center (EPIC) (Hughes Aircraft Co., Culver City, Colo.) publishes similar memorandums that include optical properties (absorption, reflection, and refractive index) of semiconductors. TPRC, DMIC, and EPIC publish summary reports, glossaries, and data sheets as sufficient information is evaluated and compiled. Listings of publications and services are available by writing to these organizations.

Energy Transmission Losses

The most common causes of energy loss between source and pyrometer are the presence of windows, magnifying lenses, prisms, and mirrors. These items are temperature error producing nuisances aggravated by the occurrence of thin films from either dirty or evaporating hot sources.

Probably the best method of determining the transmission of the optical system between source and pyrometer is by direct measurement. Often this can be done by using a calibration apparatus (figs. 10 or 11, pp. 18 and 21, respectively) containing brackets on which the windows, for instance, can be mounted. Pyrometer sightings, $S_{B,1}$ and $S_{B,2}$, respectively, are made on the target with and without the window in place, by interpreting equation (D4) as

$$\frac{1}{S_{B,2}} = \frac{1}{S_{B,1}} + \frac{\lambda}{C_2} \ln \tau' \tag{25}$$

Values of transmission τ' can be obtained directly from the temperature conversion charts (fig. 30, pp. 56 to 61) by replacing T by $S_{B,2}$, S_B by $S_{B,1}$, and ϵ' by τ'. One merit of this procedure is that τ' can be evaluated before and after one or more of the surfaces of interest has been dirtied. Also, one lumped value τ' can be applied to a group of items positioned in the optical path.

Radiation-properties data for a good quality optical device are usually provided by the manufacturer on request. The brief discussion that concludes this section of the report emphasizes the type of properties data needed for an evaluation of transmission τ'.

Mirrors for optical and scientific uses are provided by numerous manufacturers. A front-surface metallic mirror is preferred because the light undergoes only one reflection, whereas a back-surface mirror has an added reflection from the front of the glass. Because the metal is soft, manufacturers provide a thin overcoat of hard quartz to improve durability. One of the more commonly used mirrors is quartz-overcoated aluminum, the latter having been thermal evaporation deposited on glass. Generally, mirrors are spectrally selective reflectors. A typical aluminum mirror has a reflectance of 0.88 at 4000 angstroms, 0.93 at 6500 angstroms, 0.82 at 8600 angstroms, and 0.99 at 25 000 angstroms. An explanation of these variations of reflectance with wavelength lies in the presence of bound and free electrons in the metal (ref. 28).

Optical windows (also lenses and prisms) range from ordinary window glass to single-crystal oxides such as sapphire. The choice of window composition depends on many environmental factors, namely exposures to extreme conditions of temperature, pressure, chemical attack, mechanical abrasion, radiation damage, and vacuum sealing. The transmission of well-polished, clean, homogeneous windows can be evaluated from electromagnetic radiation theory provided that the proper physical constants of the material are known. Harrison (ref. 28) explains the theory in a very lucid manner, presenting first a simplified analysis for materials that have relatively large values of transmission. In this simplified analysis, the direction of radiation is taken to be within 30° of the surface normal, and the absorption coefficient k is assumed to be small. Then the transmission is shown to be closely approximated by

$$\tau' = (1 - \rho)^2 \tau \tag{26}$$

where the first term accounts for the reflection of the beam at both the front and back surfaces, and the second term is the transmittance of the window. At each surface, the reflectance ρ is expressed by

$$\rho = \left(\frac{n - 1}{n + 1}\right)^2 \tag{27}$$

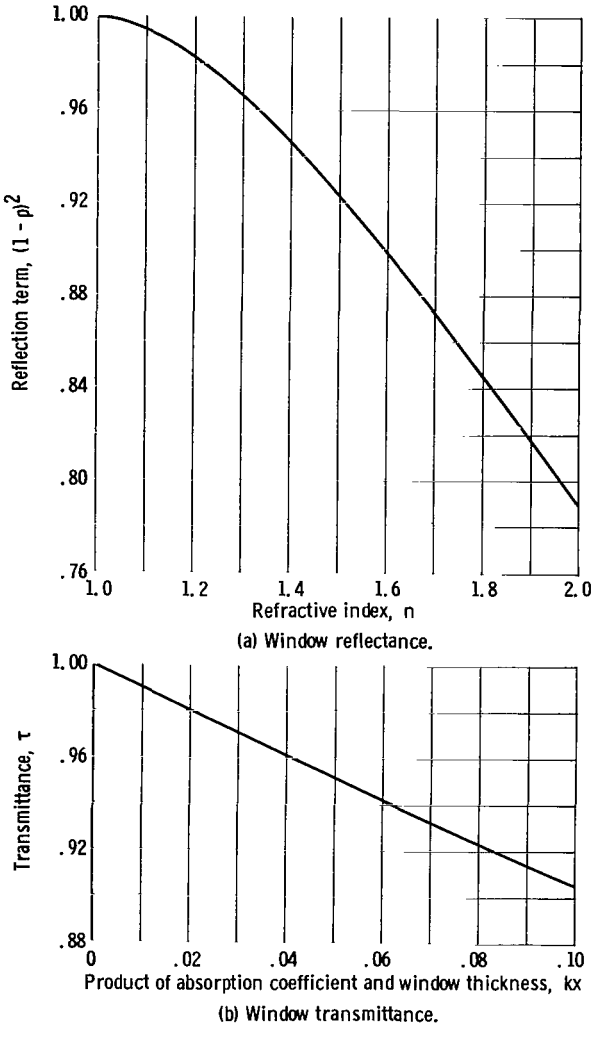

Figure 25. - Components of window transmission from equation (26).

where n, the refractive index, is the ratio of velocity of radiant energy in vacuum to its velocity in the window material. (The velocity of light has essentially the same value for air and inert gases as for vacuum.) The window transmittance in equation form is

$$\tau = e^{-kx} \tag{28}$$

where k is the absorption coefficient, and x is the window thickness. Note that kx, as well as n, is dimensionless. The two terms of equation (26) are shown in figure 25 as functions of their respective independent variables. The range of variables has been limited to the region where the equation is reasonably accurate. In review, more rigorous formulation of the transmission equation is recommended whenever

(1) The angle formed by the incident light and the surface normal exceeds 40° or

(2) n is larger than 2.0 or

(3) τ is smaller than 0.9

(See Harrison, ref. 28, or Jenkins and White, ref. 15.)

In any contemplated search for values of n and k, it is well to note that properties data are sometimes presented in the form of the following dimensionless expressions

$$\kappa = \frac{k\lambda}{4\pi n} \tag{29a}$$

and

$$\kappa n = \frac{k\lambda}{4\pi} \tag{29b}$$

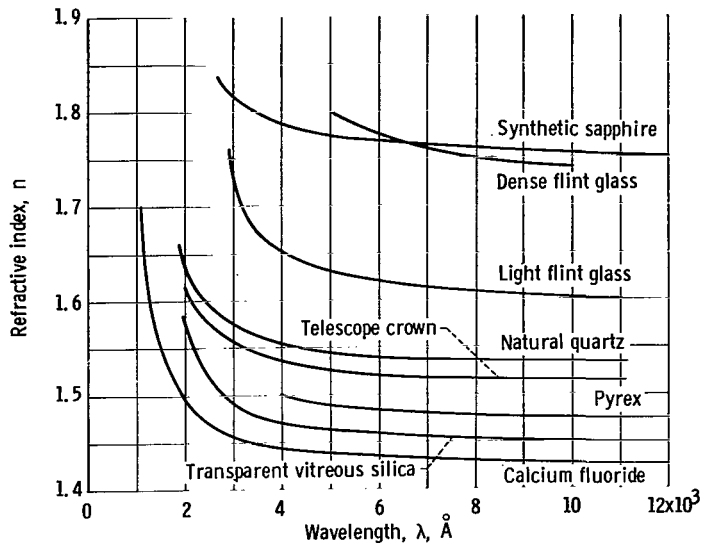

Figure 26. - Refractive index of several transparent materials at room temperature (refs. 15 and 28).

in which κ is the absorption index and, κn is the extinction coefficient.

Refractive-index data for several window materials are shown in figure 26, and absorption-coefficient data are shown in figure 27.

Values of n (fig. 26) are nearly independent of wavelength from 10 000 to 50 000 angstroms. Also, n varies only slightly with temperature; Gryvnak and Burch (ref. 29) report that the value of n for sapphire increases 0.05 unit as the temperature is increased from ambient temperature to approximately 1700° C. Absorption-coefficient data vary considerably with both wavelength and temperature and hence are shown (fig. 27) over a wide range of parameters.

A few general remarks on window materials may be helpful. A good discussion on the composition, electron-tube application, and nomenclature of various glasses is contained in reference 30, which includes a lengthy bibliography on glass. Reference 31 provides considerable data on optical properties of many glasses. The materials shown in figures 26 and 27 are briefly described as follows. Flint glasses may be defined as glasses that have a relatively large value of n. Usually they contain some lead oxide. Crown glasses possess a low value of n. Soda-lime-silica glass is a typical crown glass; by adding the appropriate oxide, one may obtain borosilicate crowns, barium crowns, etc. Corning Pyrex is a specific borosilicate crown glass. Transparent vitreous silica and quartz are composed almost entirely of silica (SiO_2). The first is an amorphous material (glass), while the second is a crystalline substance. Neither one is to be confused with "high silica glass" such as Corning Vycor, which contains about 96 percent SiO_2. (The nomenclature used herein for the SiO_2 materials has been recommended by Laufer, ref. 32.) The sapphire discussed here is a clear synthetic crystal of aluminum oxide (Al_2O_3).

For many window materials, transmission losses at wavelengths less than 20 000 angstroms are usually the result of the reflection component. That this is so can be quickly verified by inspection of the equations and figures provided herein. Reflection losses and hence reflection error are reduced markedly by commercially provided "coated" windows. A common film is composed of magnesium fluoride (MgF_2) that starts to evaporate near 300° C in vacuum.

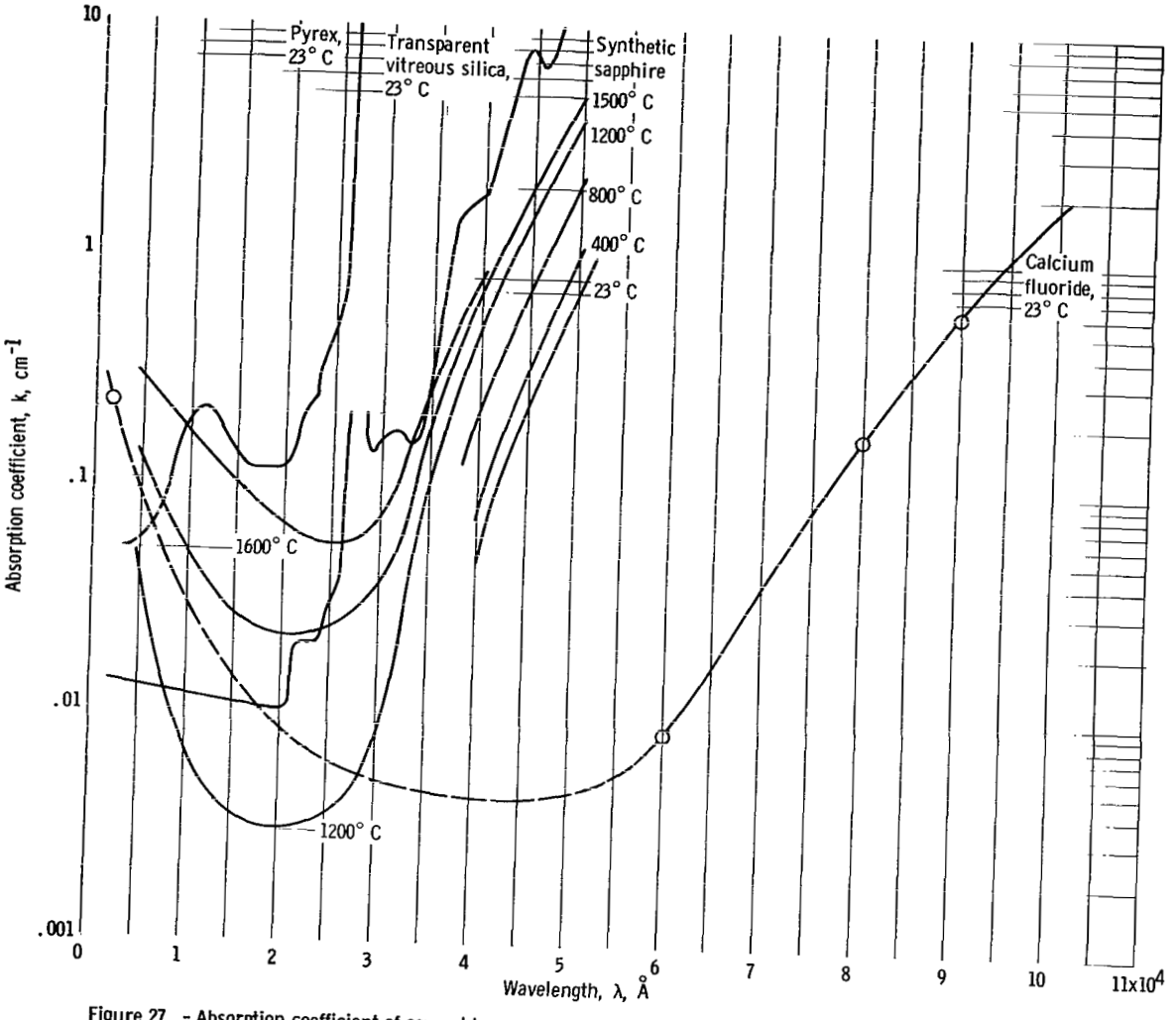

Figure 27. - Absorption coefficient of several transparent materials. Sapphire data taken from reference 29. All other data taken from reference 28.

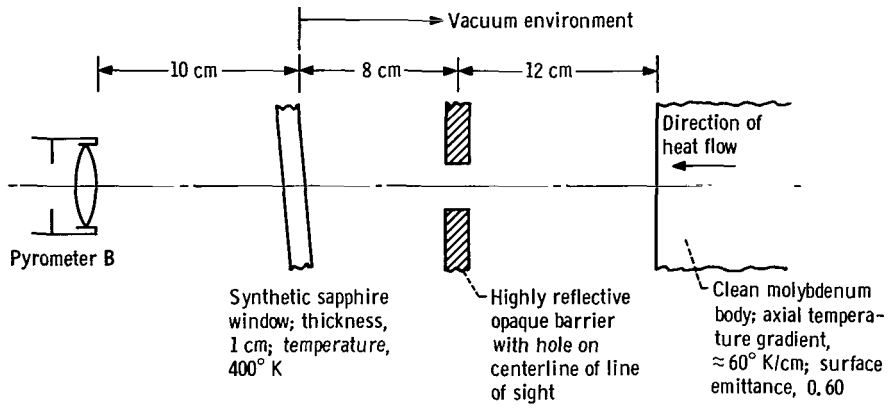

Figure 28. - Typical application using an optical pyrometer.

All glasses exposed to X-rays or gamma rays darken. Specially designed glasses for atomic shielding are described in reference 33.

ILLUSTRATIVE EXAMPLE

The diagram in figure 28 assists in highlighting several of the previously discussed facets of pyrometric applications. Multiple reflections between the body and the barrier would produce a pyrometer-indicated temperature considerably higher than the value obtained in the absence of the barrier. Hence, the presence of the barrier spurs use of the cavity technique even though the surface emittance ϵ is well defined. The sizeable temperature gradient suggests a fairly shallow cavity. Figure 21 (p. 37) shows an electrically disintegrated cavity with a length to diameter ratio of 5 to have an ϵ_a value of 0.945. Previous discussion stated that uniform brightness exists over the central two-thirds of the end-disk area. A cavity diameter D of 0.028 centimeter at a spacing of 30 centimeters is permitted (fig. 15(b)). Since the minimum error-free target diameter w (fig. 15(b)) is only 0.021 centimeter, the nonuniformly bright periphery of the end-disk is not required by the eye when a brightness match is made. The end-disk is 0.14 centimeter from the surface and is approximately 8.4° K hotter than the surface.

The minimum permissible diameter of the cavity in the barrier can be obtained from geometric considerations (fig. 13). The entrance pupil diameter d has been given as 1.42 centimeters. Hence, the cavity must possess a diameter larger than $12/30 \times 1.42$ centimeters. A 0.75-centimeter-diameter opening provides for some misalinement.

The coated window virtually eliminates all multiple reflections between the cavity and the window. Figures 25(b) and 27 indicate that window transmittance τ is near a value of 0.995. The reflection term $(1 - \rho)^2$ has a value of 0.854 (see figs. 25(a) and 26). The transmission τ' obtained from equation (26) is 0.850.

For an indicated temperature S_B of 2000° K, a true surface temperature T is obtained from equation (C2) as follows:

$$\frac{1}{T} = \frac{6530}{1.438\times10^{8}} \ln(0.945 \times 0.850) + \frac{1}{2000 - 8.4}$$

$$= 4.54\times10^{-5}(-0.219) + 50.20\times10^{-5}$$

$$T = 2033^\circ \text{ K}$$

Figure 30(a) (pp. 56 to 58) would have eliminated most of the arithmetic.

Inherent in the preceding calculations are several assumptions that bear repeating: The cavity has been properly aged and shows no marked lowering in ϵ_a values indicative of whisker growths, the window remains film-free, the influence of other radiation sources is negligible, and tolerances on cavity dimensions adhere to recommended values.

CONCLUDING REMARKS

Precision, accuracy, and speed of obtaining temperature from radiation measurements are progressively undergoing improvement. In practical applications, knowledge of the radiative properties of the target and intervening media influence accuracy as much as the quality of the pyrometer does.

In Education of a Pyromotrist (ref. 4, p. 326), R. J. Sosman stated that a good pyromotrist is also a skepticist. This advice is as timely today as when it was written 25 years ago.

Lewis Research Center,
National Aeronautics and Space Administration,
Cleveland, Ohio, March 25, 1966,
123-33-02-09-22.

APPENDIX A

GLOSSARY OF RADIANT ENERGY TERMS

pyrometer: an instrument for measuring temperatures, especially those beyond the range of mercurial thermometers

optical pyrometer: a monochromatic or pseudomonochromatic radiation pyrometer

visual optical pyrometer: an instrument that uses the human eye as a detector and hence is limited to visible radiation; often referred to as a "disappearing-filament" optical (or "brightness") pyrometer

photoelectric optical pyrometer: an instrument that uses a photoelectric detector in the visible or neighboring spectral regions; contains electronic components that usually permit direct temperature readout or record, hence it is frequently referred to as an "automatic brightness" pyrometer

ratio pyrometer: a radiation sensing pyrometer that determines temperature from the ratio of spectral radiance at two or more wavelengths in the visible or near-infrared region of radiation; frequently referred to as a "color" pyrometer; this category of instruments can use the human eye as a sensor since the eye can discern variations in both color and brightness; however, a photoelectric detector is normally employed and is the type discussed herein

total radiation pyrometer: an instrument, often referred to as a "radiation" pyrometer, that utilizes a thermoelectric or photoelectric sensor to detect a wide band of radiant energy (heat); this instrument, not a subject of this report, is described in references 2 and 28

brightness temperature: a temperature indicated by an optical pyrometer; if the pyrometer, properly calibrated, is viewing a blackbody and the line of view contains no absorbing materials, the indicated temperature equals the temperature of the viewed object

color temperature: a temperature indicated by a ratio pyrometer; if the pyrometer, properly calibrated, is viewing a blackbody or a graybody and the line of view contains only gray absorbing materials, the indicated temperature equals the temperature of the viewed object

blackbody: a radiation source that radiates at the maximum theoretical rate; a blackbody has an emittance of 1 and can absorb all the radiation incident upon it

graybody: a radiation source that radiates at a constant fraction of the blackbody radiation rate irrespective of the wavelength of the radiation

spectral radiance: the energy radiated by a body in a particular direction per unit time, per unit wavelength, per unit projected area of the body, and per unit solid angle

photometric brightness: the radiance of a body evaluated according to its capacity to produce visual sensation

emissivity: the ratio of the radiant energy emitted by the polished, damage-free surface of an opaque material to the radiant energy emitted by a blackbody source when both sources are at the same true temperature

emittance: the ratio of the radiant energy emitted by an arbitrary source to the radiant energy emitted by a blackbody source when both sources are at the same true temperature

reflectance: the ratio of the reflected radiant energy of an object to the corresponding incident radiant energy upon it

transmittance: the ratio obtained by dividing the intensity of radiation just after entering the surface of some medium into the intensity just reaching the opposite surface

transmission: the ratio obtained by dividing the intensity of radiation just before entering a medium into the intensity just after leaving the opposite surface; it is the result of two factors, the losses by reflection at the interfaces and the transmittance of the medium

spectral (also monochromatic): a description that pertains to a discrete wavelength

diffuse surface: a surface that emits or absorbs energy regardless of direction (a blackbody surface is a diffuse surface)

specular surface: a surface that reflects a beam of incident light in a mirror-like manner

APPENDIX B

SYMBOLS

C_1	first radiation constant, 1.1909×10^{-12} W/(sq cm)(steradian)
C_2	second radiation constant, 1.438 (cm)(^oK)
D	diameter of cavity entrance, cm
d	entrance pupil diameter, cm
d_f	apparent filament diameter, cm
E	correction in $1/S_B$ or in $1/S_C$, $^oK^{-1}$
k	absorption coefficient, cm^{-1}
L	depth of cavity, cm
ℓ	distance, cm
m_1, m_2	rays
N_λ, N'_λ	spectral radiance, W/(cu cm)(steradian)
n	refractive index
R	cavity radius, cm
R_o	ratio of two signals incident upon photodetector
r	position on back wall measured from cavity centerline
S	brightness or color temperature, ^oK
T	temperature, ^oK
V_λ	luminosity factor of eye
w	target diameter, cm
x	window thickness, cm
α	normal spectral absorptance
β	percent uncertainty in value of T
γ	percent uncertainty in value of ϵ
ϵ	normal spectral emittance or emissivity
ϵ_a	local cavity emittance
ϵ_c	average cavity emittance
ϵ'	effective emittance
$\bar{\epsilon}$	hemispherical total emittance
θ_f	field angle subtended by filament diameter, rad
θ_o	theoretical image resolution angle, rad
θ_t	field angle subtended by target, rad
κ	absorption index
λ	wavelength, cm (unless stated as Å)
ρ	spectral reflectance
τ	normal spectral transmittance
τ'	normal spectral transmission of a medium or system

Subscripts:

B	associated with brightness temperature
b	blackbody
C	associated with color temperature
G	gold point (melting point)
p, q	values of wavelength
1, 2	denotes different locations or wavelengths

APPENDIX C

CHARTS OF BRIGHTNESS AND COLOR TEMPERATURES

In the derivation and discussion of equations (9) and (13), it was assumed that the pyrometer had an unhindered view of a source whose emittance was known. Usually, an absorbing and/or reflecting medium exists between the source and the pyrometer. Hence, only a fraction of the energy beamed toward the pyrometer reaches it. At any given wavelength interval, this fraction has been defined for this report as the transmission τ' of the system. Therefore, the symbol ϵ in equations (9) and (13) should be replaced by

$$\epsilon' = \epsilon\tau' \tag{C1}$$

where ϵ is the emittance of the source, and ϵ' is the effective source emittance. Equations (9) and (13), which now become

$$\frac{1}{T} = \frac{1}{S_B} + \frac{\lambda}{C_2} \ln \epsilon' \tag{C2}$$

$$\frac{1}{T} = \frac{1}{S_C} - \frac{\lambda_1\lambda_2}{C_2(\lambda_1 - \lambda_2)} \ln \frac{\epsilon'_1}{\epsilon'_2} \tag{C3}$$

were used to prepare charts so that the true temperature could be easily obtained from the temperature readout of a calibrated pyrometer for systems of known ϵ'. The charts (figs. 29 and 30) present the color temperature corrections and brightness temperature corrections.

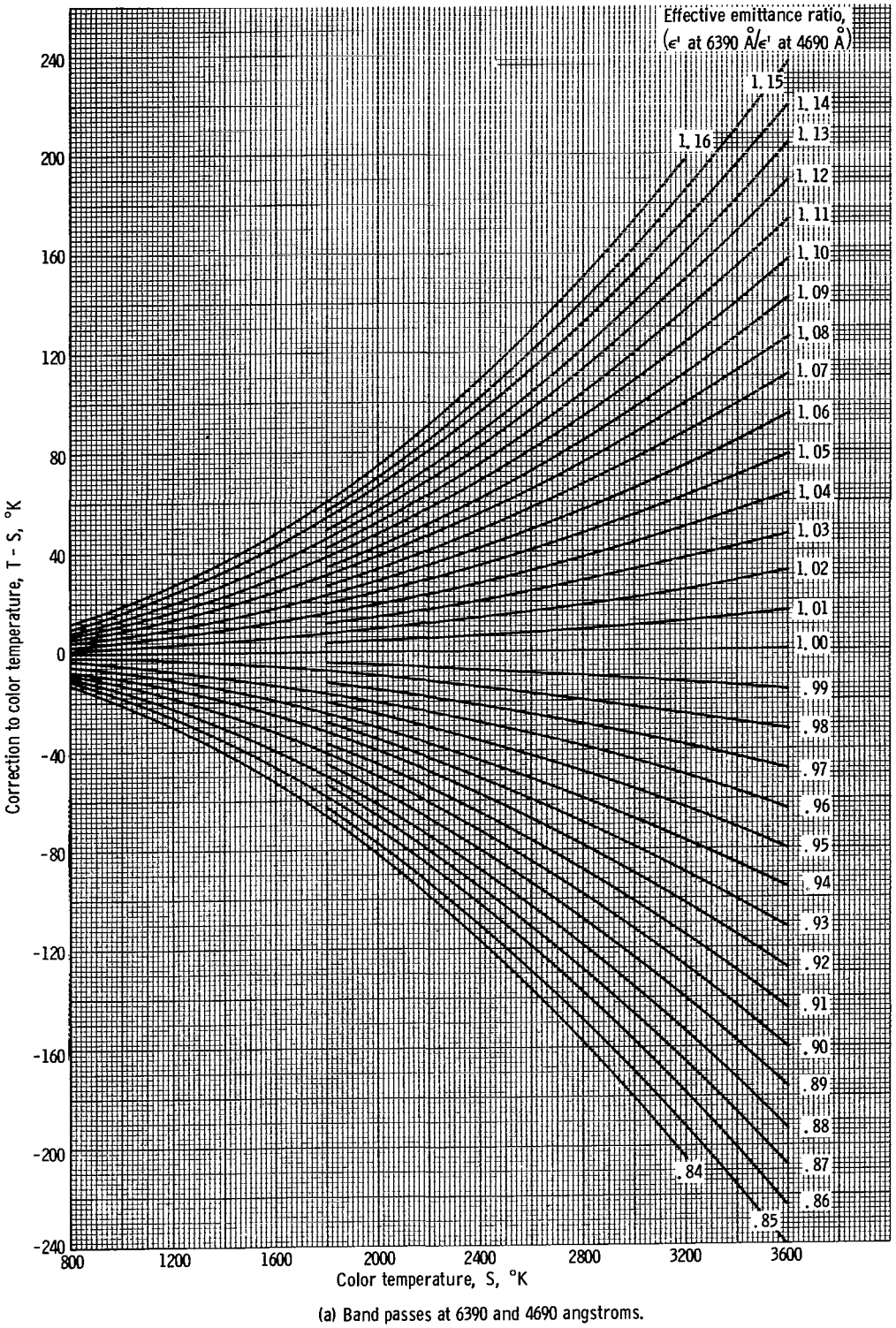

(a) Band passes at 6390 and 4690 angstroms.

Figure 29. - Color-temperature correction for a ratio pyrometer.

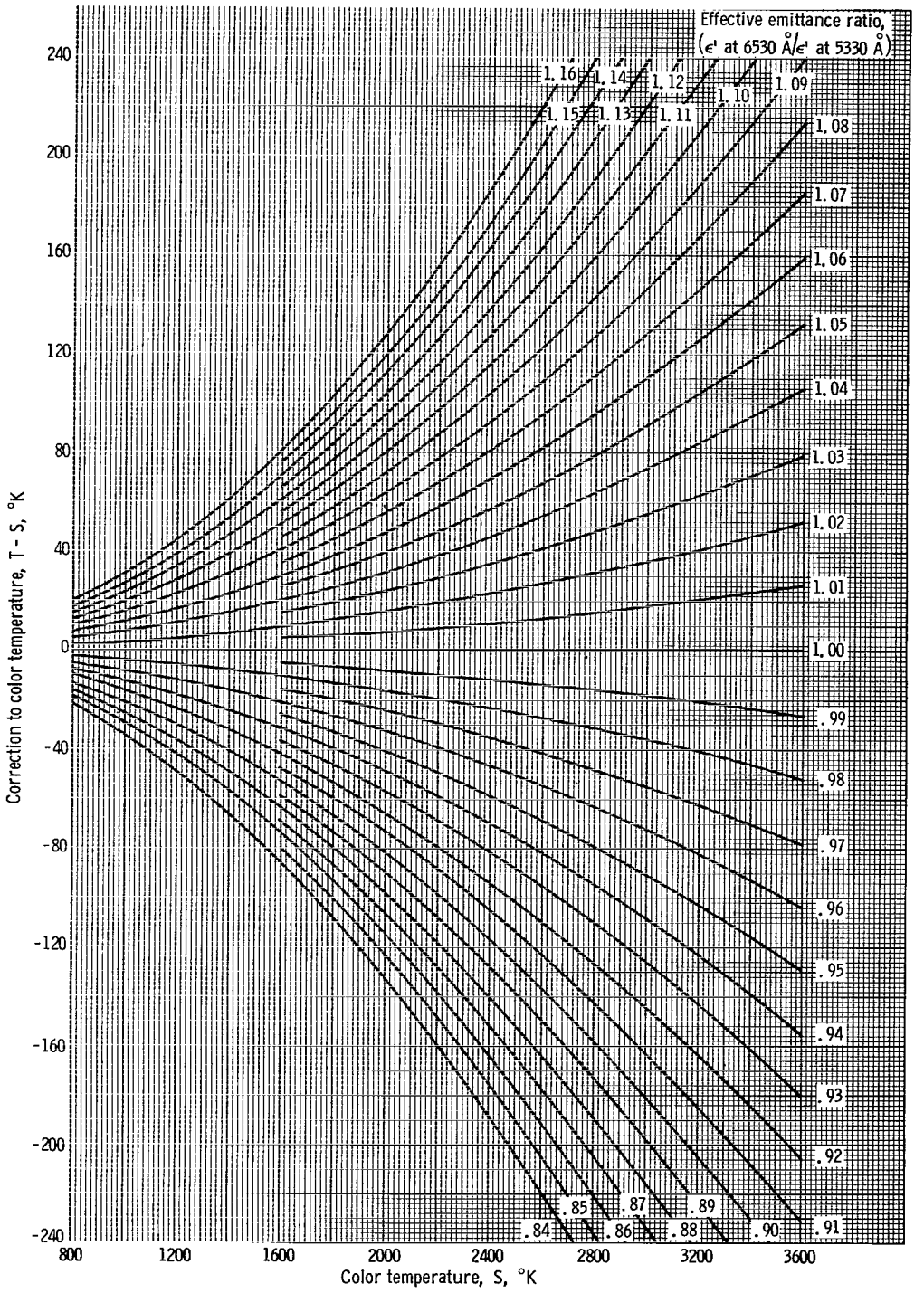

(b) Band passes at 6530 and 5330 angstroms.

Figure 29. - Concluded.

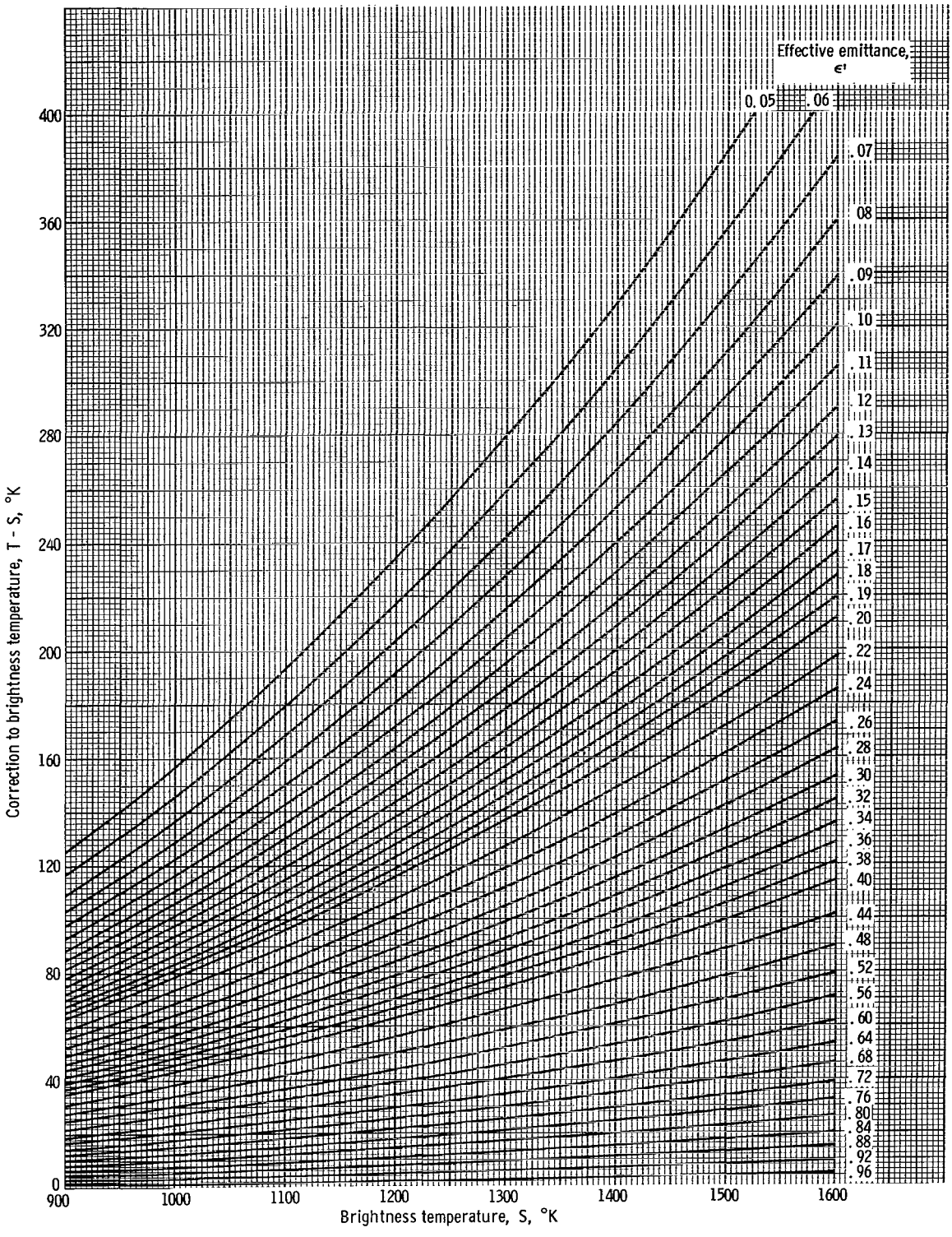

(a) Band pass at 6530 angstroms.

Figure 30. - Brightness temperature correction for an optical pyrometer.

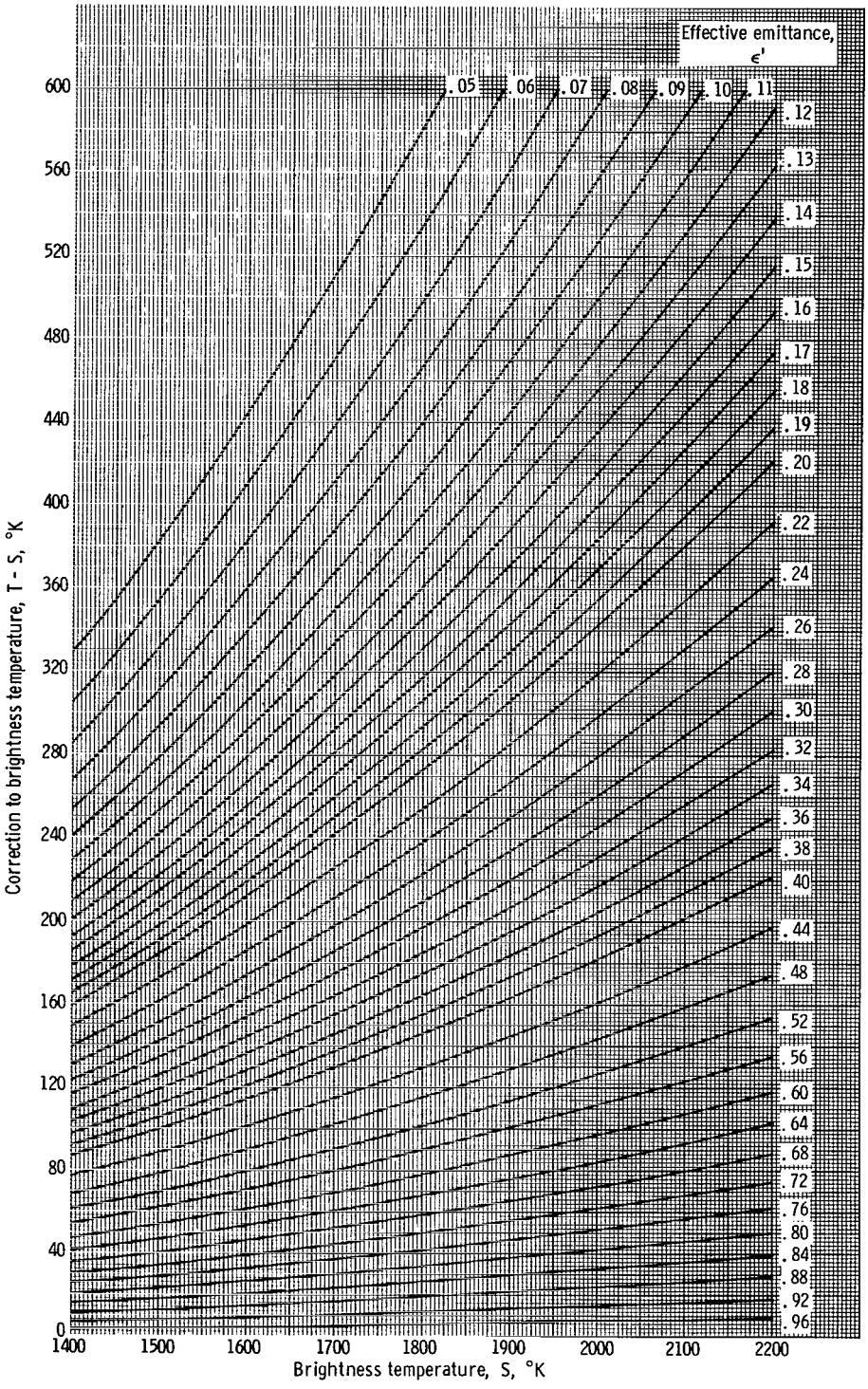

(a) Continued.

Figure 30. - Continued.

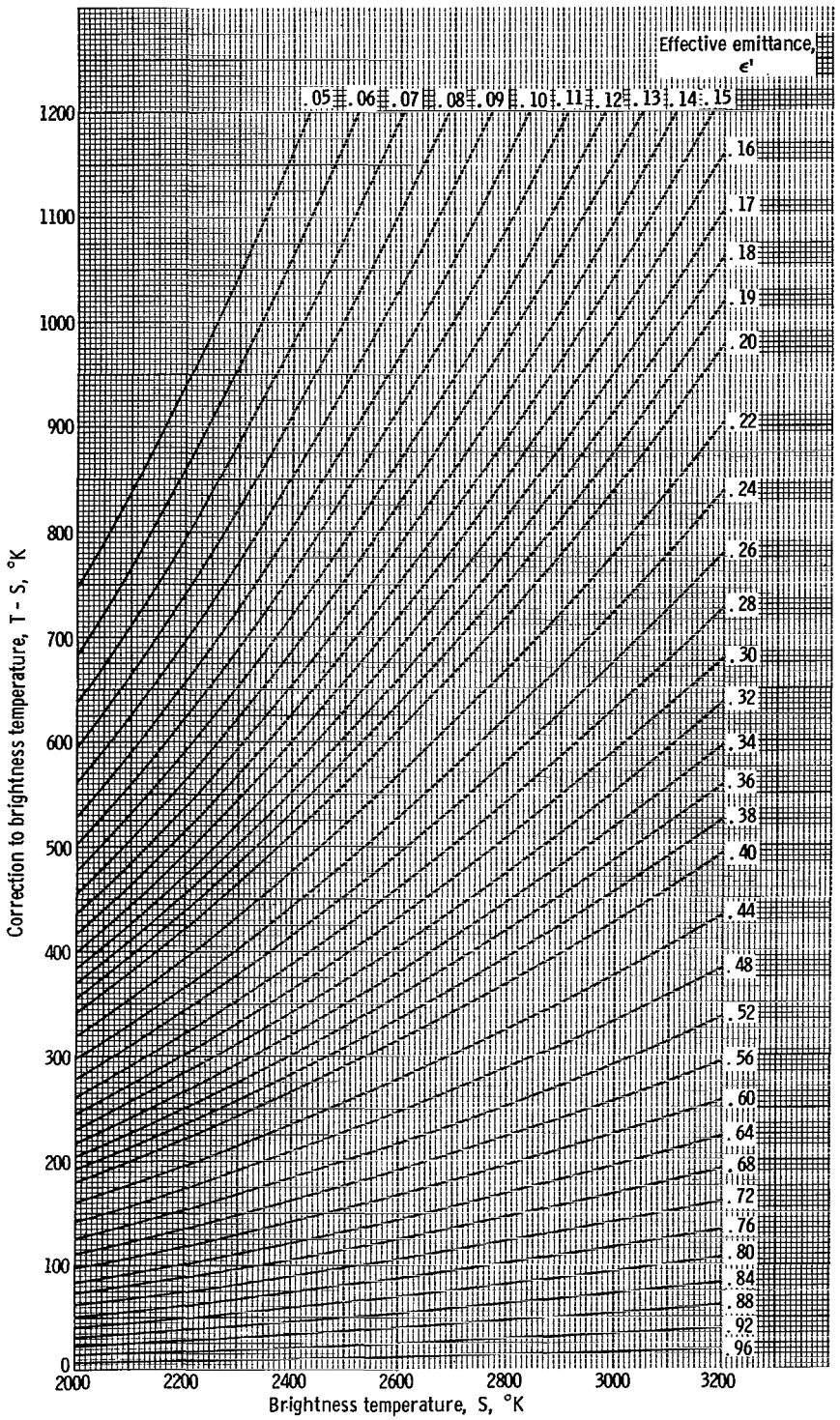

(a) Concluded.

Figure 30. - Continued.

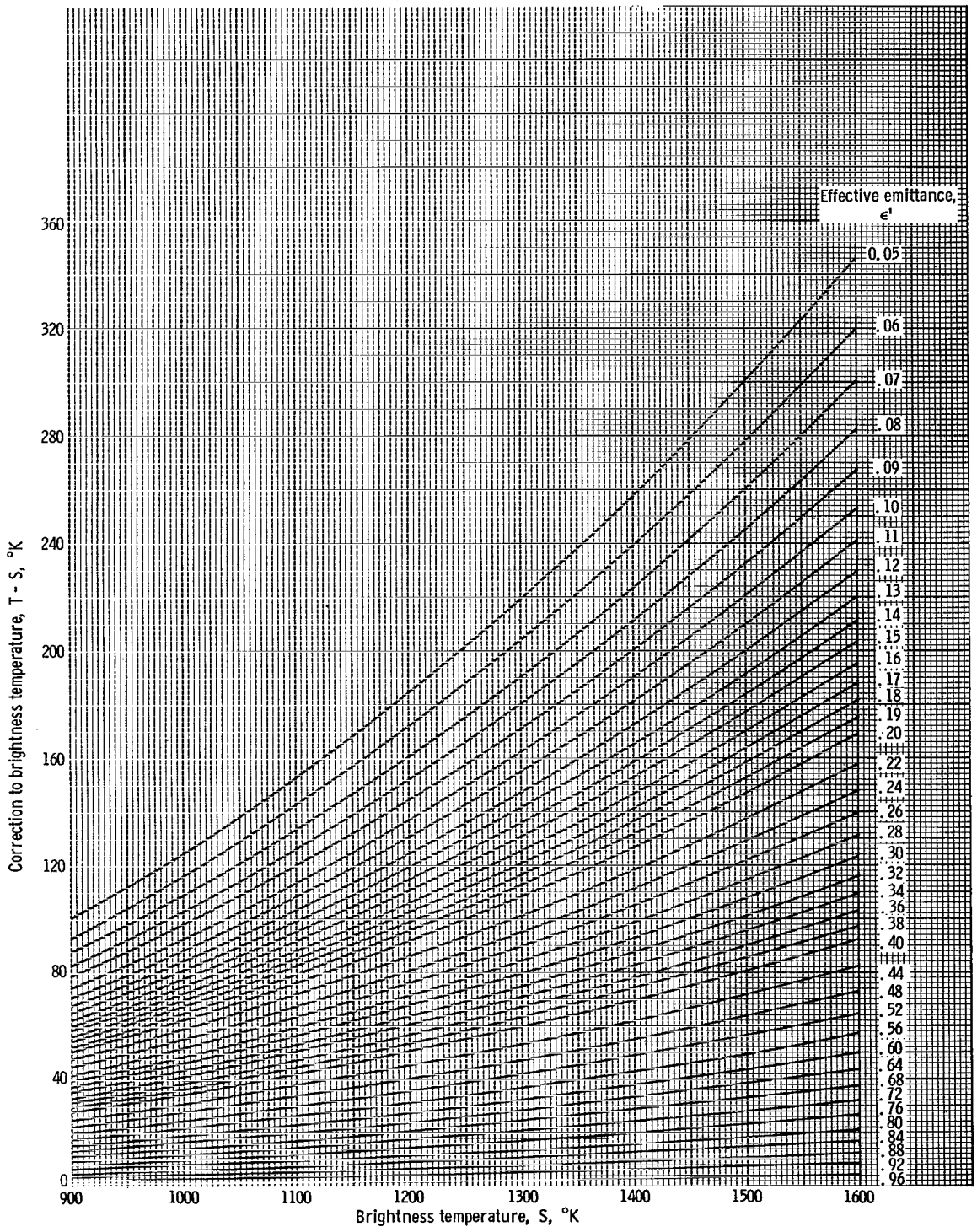

(b) Band pass at 5330 angstroms.

Figure 30. - Continued.

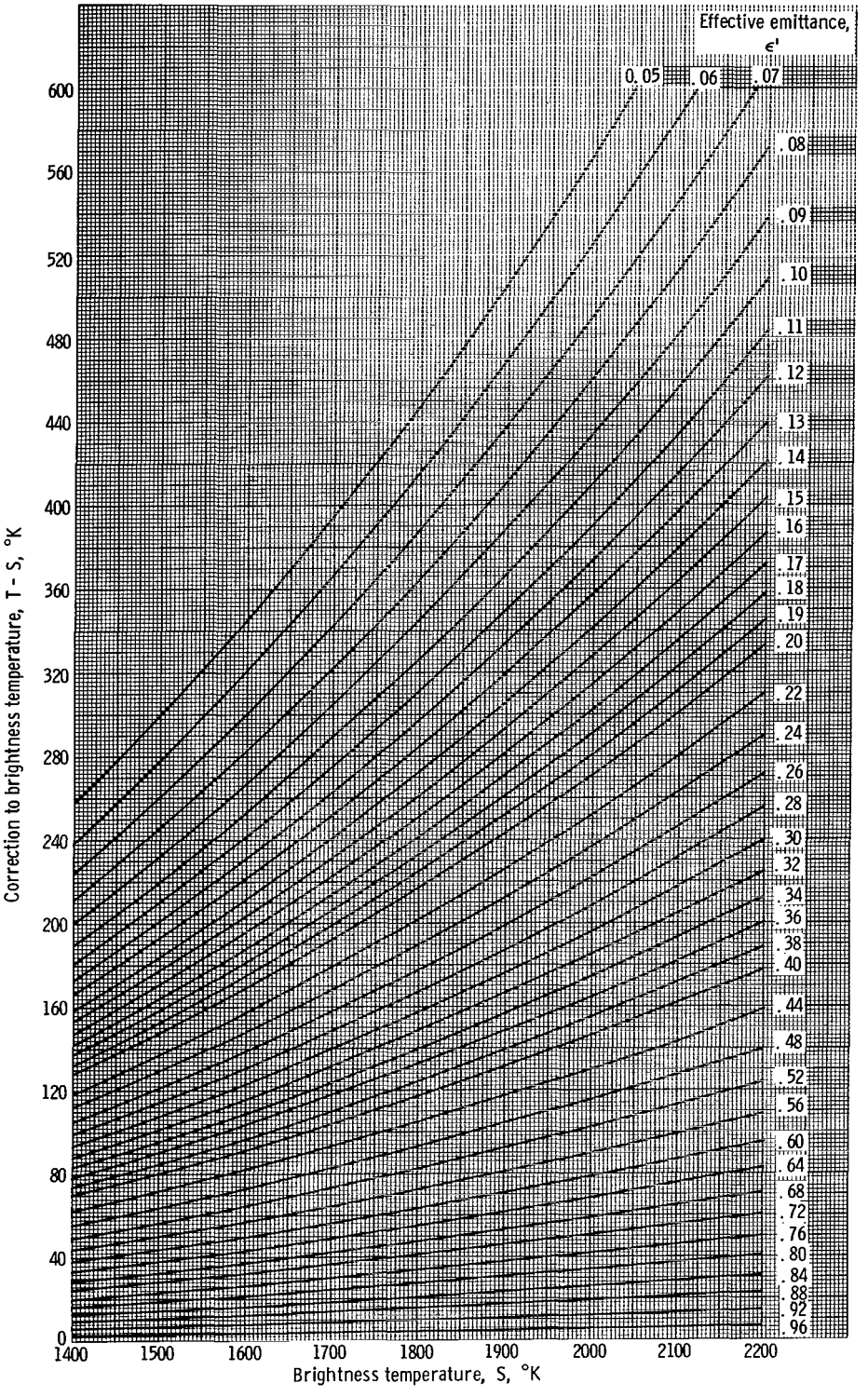

(b) Continued.

Figure 30. - Continued.

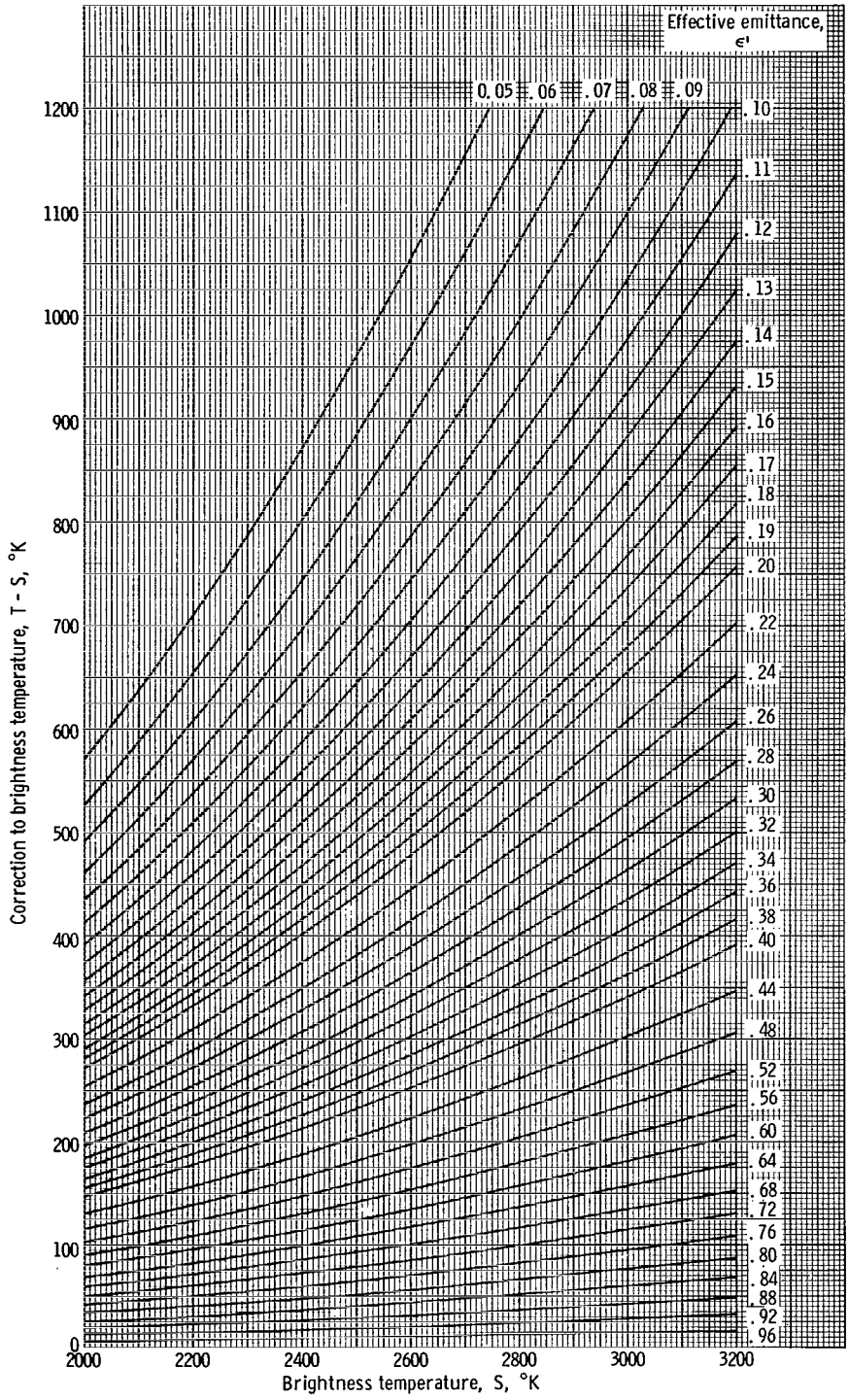

(b) Concluded.

Figure 30. - Concluded.

APPENDIX D

CAVITY EMITTANCE APPARATUS, CAVITY FABRICATION, AND COMPUTATIONAL PROCEDURE

Spectral emittance measurements were obtained for a limited variety of small cavities, and the results are presented in the text. Cavities were drilled into the ends of metal rods (figs. 31 to 33). Each rod was induction-heated in a high-vacuum chamber (fig. 33) and the entire, polished rod-end containing the cavities was radiated to "space." Front surface and cavity temperature readings were obtained with an optical pyrometer at 6530 angstroms along the cavity axis and through a window that had a remotely operated shutter, which kept contaminants from reaching the window. Multiple reflections between window and rod-end were minimized by locating the window normal slightly off-angle to the axis of the rod. Nearly all other stray radiation was captured by the chamber walls and the induction coil.

Rods of tungsten and molybdenum were chosen because (1) both can be heated to high temperatures, a requirement for good accuracy and for evaluation of the influence of temperature gradients, and (2) their respective smooth-surface emittance values differ considerably. Drilling by electrical disintegration yielded cavities of fairly uniform surface texture. Cones and cylinders were fabricated. The cavities were out-of-round by

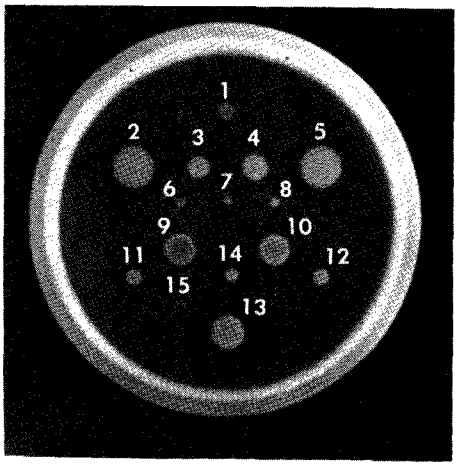

CS-37439

Cylinders

	Diameter, mm	Length to diameter ratio,
6	0.27	0.80
7	.27	1.55
8	.30	2.39
14	.40	4.85
1	.49	.85
11	.50	2.00
12	.50	3.10
9	1.00	1.04
10	1.00	2.06
13	1.00	3.10

Cones

	Diameter, mm	Angle, deg
3	0.80	42
4	.90	24
2	1.40	34
5	1.40	18

15 Control surface (Roughened by drill)

Figure 31. - Tungsten rod-end; temperature, 1500° K.

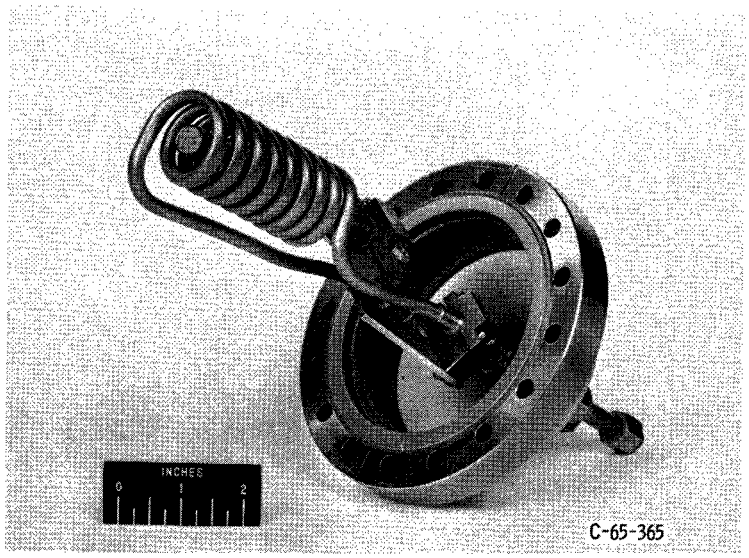

Figure 32. - Cavity emittance specimen mounted within induction coil.

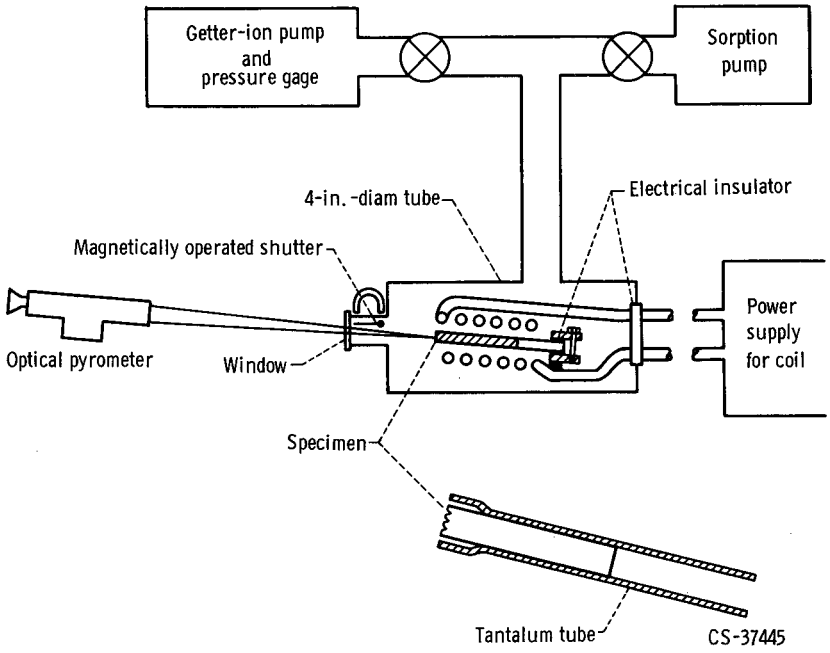

Figure 33. - Apparatus for measuring cavity emittance.

approximately 0.002 centimeter. The radius of curvature was about 0.005 centimeter for the cone apexes and for the corners of the cylinders. Frequent dressing and replacement of the electrodes used in the drilling process were required to obtain these tolerances.

Computation of cavity emittance assumed that the normal spectral emittance ϵ_1 of the polished face of the rod was known. The true temperature of the front face of the rod can be obtained from equation (C2) that now becomes

$$\frac{1}{T} = \frac{\lambda}{C_2} \ln \epsilon_1' + \frac{1}{S_{B,1}} \tag{D1}$$

where $S_{B,1}$ is the brightness temperature of the surface, and ϵ_1' is the product of ϵ_1 and τ', the window transmission. Likewise, the true temperature of the metal front-face is described by

$$\frac{1}{T} = \frac{\lambda}{C_2} \ln \epsilon_2' + \frac{1}{S_{B,2}} \tag{D2}$$

where $S_{B,2}$ is the brightness temperature of the cavity (after subtraction of ΔT, the estimated temperature difference between the back wall of the cavity and the front-face of the rod), and ϵ_2' is the product of cavity emittance ϵ_2 and τ'. Equating the two expressions for $1/T$ yields

$$\frac{1}{S_{B,2}} = \frac{1}{S_{B,1}} + \frac{\lambda}{C_2} \ln \frac{\epsilon_1'}{\epsilon_2'} \tag{D3}$$

which, in this case, is identical to

$$\frac{1}{S_{B,2}} = \frac{1}{S_{B,1}} + \frac{\lambda}{C_2} \ln \frac{\epsilon_1}{\epsilon_2} \tag{D4}$$

(In the section CAVITY EMITTANCE ϵ_c and/or ϵ_a are used in place of ϵ_2.) Comparison of equations (D4) and (C2) shows an analogy between T and $S_{B,2}$, between S_B and $S_{B,1}$, and between ϵ' and ϵ_1/ϵ_2. Hence, values of ϵ_1/ϵ_2 can be obtained directly from the brightness temperature charts (fig. 30) for experimentally obtained values of $S_{B,2}$ and $S_{B,1}$.

REFERENCES

1. Brickwedde, F. G., ed.: Temperature - Its Measurement and Control in Science and Industry. Vol. 3, Pt. I: Basic Concepts, Standards and Methods. Reinhold Pub. Corp., 1962.

2. Dahl, A. I., ed.: Temperature - Its Measurement and Control in Science and Industry. Vol. 3, Pt. 2: Applied Methods and Instruments. Reinhold Pub. Corp., 1962.

3. Kostkowski, H. J.; and Lee, R. D.: Theory and Methods of Optical Pyrometry. Monograph No. 41, NBS, 1962. (See also ref. 1, pp. 449-481.)

4. Anon.: Temperature - Its Measurement and Control in Science and Industry. Reinhold Pub. Corp., 1941.

5. Stimson, H. F.: The International Practical Temperature Scale of 1948. J. Res. Nat. Bur. Std., vol. 65A, no. 3, May-June 1961, pp. 139-145. (See also J. Res. Nat. Bur. Std., vol. 42, no. 3, Mar. 1949, pp. 209-217.)

6. Stimson, H. F.: Heat Units and Temperature Scales for Calorimetry. Am. J. Phys., vol. 23, no. 9, Dec. 1955, pp. 614-622.

7. Pivovonsky, Mark; and Nagel, Max R.: Tables of Blackbody Radiation Functions. Macmillan Co., 1961.

8. Pyatt, E. C.: Some Consideration of the Errors of Brightness and Two-Colour Types of Spectral Radiation Pyrometer. Brit. J. Appl. Phys., vol. 5, July 1954, pp. 264-268.

9. Kogan, A. V.: A Method of Reducing the Error of a Disappearing-Filament Pyrometer. High Temperature, vol. 1, no. 2, Sept.-Oct. 1963, pp. 273-275.

10. Richmond, Joseph C., ed.: Measurement of Thermal Radiation Properties of Solids. NASA SP-31, 1963.

11. Hankins, M. A.: The Pyrometric Molarc Radiation Standard at 3800° K. Paper presented at Temperature Measurements Soc. Conf., Los Angeles (Calif.), July 17, 1962. (Available from Mole-Richardson Co., Hollywood, Calif.)

12. Katzoff, S., ed.: Symposium on Thermal Radiation of Solids. NASA SP-55 (Air Force ML-TDR-64-159), 1965.

13. Metzler, Allen J.; and Branstetter, J. Robert: Fast Response, Blackbody Furnace for Temperatures up to 3000° K. Rev. Sci. Instr., vol. 34, no. 11, Nov. 1963, pp. 1216-1218.

14. Barber, C. R.: Factors Affecting the Reproducibility of Brightness of Tungsten Strip Lamps for Pyrometer Standardization. J. Sci. Instr. vol. 23, no. 10, Oct. 1946, pp. 238-242.

15. Jenkins, Francis A.; and White, Harvey E.: Fundamentals of Optics. McGraw-Hill Book Co., Inc., 1957.

16. DeVos, J. C.: Evaluation of the Quality of a Blackbody. Physica, vol. 20, 1954, pp. 669-689.

17. Edwards, David F.: The Emissivity of a Conical Black Body. Rept. No. 2144-105-T, Eng. Res. Inst., Univ. of Michigan, Nov. 1956.

18. Sparrow, E. M.; Albers, L. U.; and Eckert, E. R. G.: Thermal Radiation Characteristics of Cylindrical Enclosures. J. Heat Transfer (Trans. ASME), ser. C, vol. 84, no. 1, Feb. 1962, pp. 73-81.

19. Polgar, Leslie G.; and Howell, John R.: Directional Thermal-Radiative Properties of Conical Cavities. NASA TN D-2904, 1965.

20. Jakob, Max: Heat Transfer. Vol. I. John Wiley & Sons, Inc., 1949.

21. Khrustalev, B. A.; Kolchenogova, I. P.; and Rakov, A. M.: Spectral Coefficients of Tantalum, Molybdenum and Niobium Radiation. High Temperature, vol. 1, no. 1, July-Aug. 1963, pp. 13-18.

22. Edwards, D. K.; and Catton, Ivan: Radiation Characterization of Rough and Oxidized Metals. Advances in Thermophysical Properties at Extreme Temperatures and Pressures, S. Grotch, ed., ASME, 1965, pp. 189-199.

23. Petrov, V. A.: Chekhovskoi, V. Ya.; and Sheinblin, A. E.: Experimental Determination of the Integral Emissivity of Metals and Alloys at High Temperatures. High Temperature, vol. 1, no. 1, July-Aug. 1963, pp. 19-23.

24. Gubareff, G. G.; Janssen, J. E.; and Torborg, R. H.: Thermal Radiation Properties Survey. Second ed., Minneapolis Honeywell Regulator Co., 1960.

25. Anon.: Data Book. Thermophysical Properties Res. Center, Purdue Univ.

26. Goldsmith, Alexander; Waterman, Thomas E.; and Hirschhorn, Harry J.: Thermophysical Properties of Solid Materials. Rept. No. 58-476, Vols. 1-5, WADD, 1960-1961. (See also Thermophysical Properties of Solid Materials by A. Goldsmith, T. E. Waterman and H. J. Hirschhorn, Vols. 1-5, Pergamon Press, 1961.)

27. Anon.: Annual Report of the Thermophysical Properties Research Center for the Period Jan. 1, 1964 to Dec. 31, 1964. Purdue Univ., 1964.

28. Harrison, Thomas R.: Radiation Pyrometry and Its Underlying Principles of Radiant Heat Transfer. John Wiley & Sons, Inc., 1960.

29. Gryvnak, David A.; and Burch, Darrell E.: Optical and Infrared Properties of Al_2O_3 at Elevated Temperatures. J. Opt. Soc. Am., vol. 55, no. 6, June 1965, pp. 625-629.

30. Kohl, Walter H.: Materials and Techniques for Electron Tubes. Reinhold Pub. Corp., 1960.

31. Morey, George W.: The Properties of Glass. Second ed., Reinhold Pub. Corp., 1954.

32. Laufer, Jerome S.: High Silica Glass, Quartz, and Vitreous Silica. J. Opt. Soc. Am., vol. 55, no. 4, Apr. 1965. pp. 458-460.

33. Anon.: Corning Radiation Shielding Windows. Rept. No. PE-51, Corning Glass Works, 1960.

"The aeronautical and space activities of the United States shall be conducted so as to contribute . . . to the expansion of human knowledge of phenomena in the atmosphere and space. The Administration shall provide for the widest practicable and appropriate dissemination of information concerning its activities and the results thereof."

—NATIONAL AERONAUTICS AND SPACE ACT OF 1958

NASA SCIENTIFIC AND TECHNICAL PUBLICATIONS

TECHNICAL REPORTS: Scientific and technical information considered important, complete, and a lasting contribution to existing knowledge.

TECHNICAL NOTES: Information less broad in scope but nevertheless of importance as a contribution to existing knowledge.

TECHNICAL MEMORANDUMS: Information receiving limited distribution because of preliminary data, security classification, or other reasons.

CONTRACTOR REPORTS: Technical information generated in connection with a NASA contract or grant and released under NASA auspices.

TECHNICAL TRANSLATIONS: Information published in a foreign language considered to merit NASA distribution in English.

TECHNICAL REPRINTS: Information derived from NASA activities and initially published in the form of journal articles.

SPECIAL PUBLICATIONS: Information derived from or of value to NASA activities but not necessarily reporting the results of individual NASA-programmed scientific efforts. Publications include conference proceedings, monographs, data compilations, handbooks, sourcebooks, and special bibliographies.

Details on the availability of these publications may be obtained from:

SCIENTIFIC AND TECHNICAL INFORMATION DIVISION

NATIONAL AERONAUTICS AND SPACE ADMINISTRATION

Washington, D.C. 20546